Arch. Rational Mech. Anal. 187 (2008) 185–220
Digital Object Identifier (DOI) 10.1007/s00205-007-0061-9

A Model for the Formation and Evolution of Traffic Jams

F. Berthelin, P. Degond, M. Delitala & M. Rascle

Communicated by C. M. Dafermos

Abstract

In this paper, we establish and analyze a traffic flow model which describes the formation and dynamics of traffic jams. It consists of a pressureless gas dynamics system under a maximal constraint on the density and is derived through a singular limit of the Aw-Rascle model. From this analysis, we deduce the particular dynamical behavior of clusters (or traffic jams), defined as intervals where the density limit is reached. An existence result for a generic class of initial data is proved by means of an approximation of the solution by a sequence of clusters. Finally, numerical simulations are produced.

1. Introduction

Mathematical and numerical models of traffic are strongly inspired by fluid mechanical models. Roughly speaking, they can be grouped into three main categories: particle models (in the traffic flow community, referred to as 'Follow-the-Leader' models [13]), kinetic models [16, 19, 20, 23] (among which there are cellular automata models [18]) and fluid models [2, 17, 21, 22, 27]. Here, we shall mainly be concerned with fluid models and their connection with particle 'Follow-the-Leader' models.

Fluid models are based on conservation (or balance) equations for a certain number of observables of the flow. First-order fluid models consist of only one conservation equation, that of the number density of cars per unit portion of road. The flux of cars is related to the number density by a local relation called the fundamental diagram. The prototype of these models is the celebrated Lighthill–Witham model [17].

When a second balance equation is retained for, say, the mean velocity of the flow, the fluid model is referred to as a second-order model. The prototype of such a model is the Payne–Whitham model [21, 22]. This kind of model mimics the

isentropic Euler system of fluid mechanics which consists of conservation equations for the number and momentum densities. However, cars in traffic have properties usual fluids do not have and, in a celebrated paper [11] DAGANZO pointed out a certain number of absurdities that appear if one tries to apply the fluid mechanical formalism to traffic flow too bluntly. Recently, AW and RASCLE [2] proposed a new second-order model (in this work referred to as the Aw-Rascle or AR model) which remedies the deficiencies pointed out by Daganzo. This model has been independently derived by ZHANG [27]. In [1], a derivation of this model from a microscopic Follow-the-Leader (FL) model through a scaling limit is given.

The present work is based on the AR model. Its starting point is the observation that, in the AR model, upper bounds on the density are not necessarily preserved through the time evolution of the solution. In practice, the density of cars is bounded from above by a maximal density n^* corresponding to a bumper to bumper situation. However, the AR model does not exclude cases where, depending on the smallest invariant region which contains the initial data, solutions satisfy the maximal density constraint $n \leqq n^*$ initially but evolve in finite time to a state, still uniformly bounded, but which violates this constraint. In the present work our first goal is to cure this deficiency. For this purpose, we assume that the velocity offset (that is the "pseudo-pressure" by analogy with fluid-mechanical models) becomes infinite as the density of cars approaches this maximal density. Our second aim is to construct an asymptotic limit in which the density is either 0 (vacuum) or $n*$ (jam) or any value strictly comprised between 0 and n^* (free traffic).

The pseudo-pressure $p(n)$ can be viewed either as a preferred velocity at any given density n, or as a velocity offset that is as the difference between the 'preferred velocity' w at vacuum (the velocity that a driver would choose if the road was totally empty) and its actual velocity u. In any case, the important feature is that w is a Lagrangian variable. In the AR model, p is a function of the local density n (like the pressure in isentropic models of gas dynamics). The function $p(n)$ is increasing because drivers reduce their velocity by a larger amount as traffic becomes denser. In the standard AR model, there is no a priori bound on the density n and $p(n)$ tends to infinity as n tends to infinity. In our Modified AR model (or MAR model), $p(n)$ tends to infinity as the n tends to the maximal density n^*. The physical background of this assumption will be discussed in Section 2. We just note that the singularity of $p(n)$ as $n \to n^*$ preserves the local bound $n \leqq n^*$ at future times.

The velocity offset is related to the velocity at which perturbations of traffic in front propagate backwards through the reactions of the drivers. In our MAR model, this propagation velocity also tends to infinity as the n tends to n^*. This can be understood as follows. In normal (uncongested) traffic, this information travels rather slowly compared with the velocity of the traffic because drivers adjust smoothly to the variations of traffic in front. In congested traffic however, the driver's reaction time is shorter and this propagation velocity becomes large.

Of course, the assumption that $p(n) \to \infty$ as $n \to n^*$ is an idealization of reality. It has interesting consequences however if one assumes further that the velocity offset is infinitesimally small as long as traffic is uncongested but becomes suddenly large when the traffic reaches a congested state. The main goal of this paper is to study this limiting situation and to show that the so-obtained model

may be useful for the description of the formation and the evolution of jams or car clusters.

Indeed, we show that this limiting situation leads to a very simple model in uncongested situations: the so-called pressureless gas dynamics (PGD) model. It consists of the conservation equation for the car density supplemented by the Burgers equation for the velocity. The latter expresses that the velocity is passively transported by itself. It is well known that the PGD model develops shocks for the velocity, and correspondingly, delta measure singularities for the density. However here, the model is constrained by the maximal density constraint and cannot exhibit such concentrations. When the density reaches the maximal density constraint, that is in congested situations, cars are then forced to spread into clusters. Their evolution is described by a degenerate form of the AR model in which the velocity offset becomes the Lagrange multiplier of the maximal density constraint.

The goal of this paper is to investigate this 'constrained pressureless gas dynamics' system (CPGD). The outline of the paper is as follows. In Section 2, we present the AR model, summarize its main properties and motivate our modification of the velocity offset p. In Section 3, after rescaling the AR system with modified p, we derive the CPGD system.

This formal derivation motivates a detailed analysis of the solutions to the Riemann problem for the CPGD system, which unfortunately has to consider many different cases and therefore could be slightly hard to read. For this reason, we have postponed it until Section 6. The reader can first skip this Section, whose main results are summarized in Section 6.4.1, but it is very instructive, and it has been a strong motivation for writing this paper. In particular, we emphasize some cartoons like cases BIII and DIII, which provide excellent prototypes of particular solutions (of clusters, or traffic jams) for both the theoretical and numerical results in the following Sections.

In Section 4, the description of cluster dynamics allows us to construct solutions of the CPGD system for generic initial data and consequently, to prove the existence of weak solutions. Then, in Section 5, we show some numerical solutions of the CPGD model, before the above-mentioned Section 6 and the Conclusion.

Other kinds of constrained pressureless gas dynamics systems have been obtained and studied in [6] (to model the dynamics of gas occlusions in pipes) and in [3, 4]. In the present case, the cluster dynamics are different. However, the mathematical techniques used in Section 4 are close, and we will highlight the points which are specific to the present case.

2. The modified AR model

Let $n(x,t)$ denote the density of vehicles, i.e. the number of vehicles per unit stretch of road, and $u(x,t)$ their velocity, as a function of the position $x \in \mathbb{R}$ and the time $t > 0$. The AR model has the form

$$\partial_t n + \partial_x(nu) = 0, \tag{1}$$

$$(\partial_t + u\partial_x)(u + p(n)) = 0, \tag{2}$$

where $p(n)$ is the velocity offset. Equivalently, exploiting the conservation of mass to simplify the velocity equation (2), we have (at least for smooth solutions)

$$\partial_t n + \partial_x(nu) = 0, \tag{3}$$

$$\partial_t u + u\partial_x u = np'(n)\partial_x u, \tag{4}$$

where p' denotes the derivative of p with respect to n. The velocity $np'(n)$, describes how drivers react to information about the state of traffic in front of them. The velocity offset p bears analogies with the pressure in fluid dynamics (in spite of the different physical dimension): it is associated with the propagation of flow perturbations of the same kind as acoustic perturbations. However, these perturbations only propagate backwards to the flow direction, as they should (see for example the detailed discussion in [1, 2]).

This model can be derived from particle models (called 'follow-the-leader' (FL) in the traffic engineering literature) as shown in [1]. The FL model treats vehicles as independent particles labeled by $i \in \mathbb{Z}$ with time-dependent positions $x_i(t)$ and velocities $u_i(t)$. The evolution of each individual vehicle is ruled by the following differential system

$$\dot{x}_i = u_i, \quad \dot{u}_i = C\frac{u_{i+1} - u_i}{(x_{i+1} - x_i)^{\gamma+1}}, \tag{5}$$

where C is an appropriate constant. This model states that a driver adjusts the velocity according to that of the leading car. If its own velocity u_i is smaller than that of the leading car u_{i+1}, it accelerates, and thus $\dot{u}_i > 0$. Conversely, if it goes faster, it must decelerate, and thus $\dot{u}_i < 0$. The acceleration/deceleration process is faster if the leading car is closer, which is expressed by the power of the distance $x_{i+1} - x_i$ between the two cars, at the denominator of (5). In [1], it is shown that the velocity offset in the AR model when derived from the FL model is given by $p(n) = cn^\gamma$, where γ is the same constant as that appearing in (5) and $c = C/\gamma$. The increase of the velocity offset with the density is related to the fact that the reaction of the drivers is faster when the cars are closer. The precise choice of the constants C and γ is a matter of modeling. We shall make $c = 1$ in the remainder of the paper.

DAGANZO [11] pointed out a certain number of deficiencies of second-order models like the Payne–Whitham model [21, 22]. The AR model actually does not exhibit the same drawbacks. In particular, as demonstrated in [1, 2] the density and velocity remain non-negative, which is highly desirable for traffic flow models.

The AR system can be put in the following conservative form

$$\partial_t n + \partial_x(nu) = 0, \tag{6}$$

$$\partial_t(nw) + \partial_x(nwu) = 0, \tag{7}$$

where $w = u + p(n)$. Therefore, it falls into the general category of conservation laws

$$\partial_t U + \partial_x f(U) = 0,$$

with the vector of conserved variables U given by $U = (n, nw)$ and the flux function $f(U) = (nu, nwu)$. The jacobian matrix $A(U) = \partial_U f$ is given by

$$A(U) = \begin{pmatrix} u & n \\ 0 & u - np'(n) \end{pmatrix}. \tag{8}$$

It has eigenvalues

$$\lambda_1 = u - np'(n) \leqq \lambda_2 = u. \tag{9}$$

If the density is different from zero, λ_1 and λ_2 are distinct, and consequently the system is strictly hyperbolic.

The Riemann invariants are u and w, associated with the eigenvalues λ_1 and λ_2 respectively. Changing unknowns to the Riemann invariants allows us to diagonalize the system in the form

$$\partial_t u + (u - np'(n))\partial_x u = 0, \tag{10}$$

$$\partial_t w + u\partial_x w = 0. \tag{11}$$

The first eigenvalue λ_1 is genuinely nonlinear, and the associated simple waves are either shock waves (which correspond to braking) or rarefaction waves (which correspond to acceleration). The second eigenvalue λ_2 is linearly degenerate, and the associated contact discontinuities describe jumps in the car density which travel with the speed of the flow. This system turns out to belong to the 'Temple class' [26], i.e. is such that shocks and rarefaction curves (in the U plane) coincide.

According to (11), w is preserved along the characteristics, i.e. the solutions $X(t)$ of the differential equation $\dot{X}(t) = u(X(t), t)$. Indeed, (11) is equivalent to saying that $w(X(t), t)$ is constant in time, or $w(X(t), t) = w_0(X(0))$, where w_0 is the initial condition for w. Since $w = u$ when $n = 0$, we can intepret w as the 'preferred velocity', that is the velocity at which the driver would go if the road was totally devoid of cars. The actual velocity $u = w - p$ is reduced from the preferred value w by the amount p, i.e. p is the velocity offset between the preferred velocity and the actual velocity. This velocity offset is caused by the obligation for the driver to reduce speed because of the presence of a density n of cars on the road.

By solving (10)–(11) by the method of characteristics, we easily deduce that any bounds on the initial data (u_0, w_0) of the form

$$a \leqq u_0 \leqq b, \quad c \leqq w_0 \leqq d,$$

easily transfer into the same bounds for (u, w) at any time

$$a \leqq u(\cdot, t) \leqq b, \quad c \leqq w(\cdot, t) \leqq d.$$

In other words, any rectangular region $[a, b] \times [c, d]$ in the (u, w)-plane is an invariant region of the AR model.

In practice however, it is more natural to think in terms of bounds on the velocity (the average velocity should stay between 0 and the upper bound on the speed of

the cars u^*) and on the density (between 0 and a maximal density n^* corresponding to a bumper to bumper situation)

$$0 \leqq u(\cdot, t) \leqq u^*, \quad 0 \leqq n(\cdot, t) \leqq n^*.$$

However, such a region in the (u, w)-plane is defined by

$$\Delta_{u^*,n^*} = \left(0 \leqq u \leqq u^*, \quad 0 \leqq w - u \leqq p\left(n^*\right)\right),$$

and is not an invariant region for the AR model. This means that initial data lying in Δ_{u^*,n^*} may generate solutions which actually leave this region. Since Δ_{u^*,n^∞} is an invariant region, solutions leaving Δ_{u^*,n^*} are such that $(u - w)(x, t) > p(n^*)$ (for some (x, t)), or that $n(x, t) > n^*$, meaning that their density exceeds the maximal allowed density n^*. Therefore, the AR model exhibits some 'unphysical' features, which we intend to correct by proposing a modification of the velocity offset p. This modification will allow us to preserve the density constraint $n \leqq n^*$ at any time.

We propose a 'modified' AR model (MAR), in which the velocity offset p takes the form

$$p(n) = \left(\frac{1}{n} - \frac{1}{n^*}\right)^{-\gamma} \qquad \text{with} \quad n \leqq n^*. \tag{12}$$

The function $p(n)$ is defined for $n \leqq n^*$ and tends to infinity when $n \to n^*$, therefore making the maximal density a limit which is never reached. We assume that n^* is a fixed constant. In practice however it should depend on the velocity, since the minimal distance a driver leaves between himself and the leading car is an increasing function of the velocity. We shall investigate this case in future work and, for the sake of simplicity, concentrate now on the constant n^* case. On the other hand, when n is small, $p(n) \sim n^\gamma$ just like in the case of the standard AR model. Therefore, the modification of the offset term only affects congested situations, the modeling of noncongested situations being largely unmodified.

The modification of the offset term does not significantly alter the analytical properties of the model, and most of what has been stated previously remains true for the MAR model (for instance the form of the conservation equations (6), (7), the formulas for the eigenvalues (9) and the Riemann invariants (10)–(11)). Besides, with no substantial modification with respect to the calculations developed in [1], the MAR model can be derived as the macroscopic limit of a Modified Follow-the-Leader model (MFL) written as follows

$$\dot{x}_i = u_i, \quad \dot{u}_i = \frac{1}{\gamma} \frac{u_{i+1} - u_i}{(x_{i+1} - x_i - d)^{\gamma+1}}, \tag{13}$$

where $d = 1/n^*$ denotes the minimal distance between the cars and $x_{i+1} - x_i > d$ for all i. We can see that the acceleration becomes infinite when the distance between the cars approaches the minimal distance d, thus preventing the cars to be closer than d (provided that it is so initially).

We now introduce a scaling of the MAR model (6), (7). We suppose that the velocity offset p is very small unless the density n is very close to the maximal density n^*. Indeed, it can be observed that drivers do not reduce their speed significantly

until traffic becomes congested. This assumption can be taken into account in the MAR model simply by changing p into εp. This leads to the so-called Rescaled MAR model (or RMAR model)

$$\partial_t n^\varepsilon + \partial_x (n^\varepsilon u^\varepsilon) = 0, \tag{14}$$

$$(\partial_t + u^\varepsilon \partial_x)(u^\varepsilon + \varepsilon p(n^\varepsilon)) = 0, \tag{15}$$

with $p(n)$ given by (12).

The goal of this paper is to derive and analyze the limit $\varepsilon \to 0$ of this RMAR model. Intuitively, we can guess that the limit system will behave like a pressureless gas dynamics system as long as the density n is below the maximal density n^*. However when n reaches n^*, the pressure term becomes active so as to preserve the constraint $n \leqq n^*$. In this regime, new dynamics occur, which requires investigation. We shall show that the dynamics model the formation and evolution of clusters (i.e. traffic jams). This formal derivation is carried out in the next section.

3. The Constrained pressureless gas dynamics Model

We investigate the limit $\varepsilon \to 0$ of the RMAR model (14), (15) in more detail.

If $p(n)$ was not singular at $n = n^*$, the formal limit would be the so-called pressureless gas dynamics system (PGD)

$$\partial_t n + \partial_x (nu) = 0, \tag{16}$$

$$(\partial_t + u\partial_x)u = 0. \tag{17}$$

This is actually the formal limit of the standard AR model after rescaling (i.e. model (14), (15) with the unmodified velocity offset $p(n) = n^\gamma$). The PGD model has a few unpleasant features: it is only weakly hyperbolic (its two eigenvalues coincide with u, but the associated eigenspace is of dimension 1 only) and therefore displays a weak linear instability. The velocity u being a solution of the Burgers equation (17) develops shocks, but correlatively the density develops delta-measure concentrations. The solution can be continued in the distributional sense in different ways beyond shocks. However, there is no entropy criterion which allows us to select a physically relevant solution, which leads to a lack-of-uniqueness problem. The PGD system has been studied for example in [5].

However, the modified velocity offset (12) tends to infinity when $n \to n^*$. Therefore, if $(n^\varepsilon, u^\varepsilon)$ is a sequence of solutions of the RMAR system converging to a solution (n, u) of the CPGD system, and if $n = n^*$ at a point (x, t), the corresponding limit $\bar{p}(x, t) = \lim_{\varepsilon \to 0} \varepsilon p(n^\varepsilon)(x, t)$ may become nonzero and finite. The quantity $\bar{p}$ appears as the Lagrange multiplier of the constraint $n \leqq n^*$ and is nonzero only when the constraint is saturated, that is when $n = n^*$. We express this alternative by $(n^* - n)\bar{p} = 0$. We also note that $\bar{p}$ is always non-negative.

Therefore, the formal limit of the RMAR system (14), (15) can be written as follows

$$\partial_t n + \partial_x (nu) = 0, \tag{18}$$

$$(\partial_t + u\partial_x)(u + \bar{p}) = 0, \tag{19}$$

$$0 \leqq n \leqq n^*, \quad \bar{p} \geqq 0, \quad (n^* - n)\bar{p} = 0. \tag{20}$$

It is a constrained pressureles gas dynamics system and will be referred to below as the CPGD system.

A similar system has been proposed in [6] for the modeling of gas occlusions in pipes. Its mathematical theory has been explored in [3, 4]. However, for that system, the Lagrange multiplier term ensured momentum conservation while enforcing the constraint. Here, the Lagrange multiplier term has a different form (in particular, it appears inside a material derivative $\partial_t + u\partial_x$ rather than inside a spatial gradient) because momentum conservation is replaced by a different rule, namely the transport of the preferred velocity w. Therefore, the qualitative features of the limit model are different and the mathematical theory must be adapted accordingly.

So far, the CPGD system (18)–(20) is still ill posed, since the velocity offset $\bar{p}$ is undetermined in the situation where $n = n^*$. In order to get more information about the solution inside a cluster, we examine in more detail the limit $\varepsilon \to 0$ of the RMAR system (14), (15) when $n^\varepsilon \to n^*$. We note that the characteristic velocities λ_1^ε, λ_2^ε of the RMAR system are given by

$$\lambda_1^\varepsilon = u - \varepsilon n p'(n), \quad \lambda_2^\varepsilon = u. \tag{21}$$

We assume that $n^\varepsilon(x,t) \to n^*$ for all x in a (possibly time-dependent) interval $I(t) = [Y_L(t), Y_R(t)]$. Furthermore, we suppose that the offset term $\varepsilon p(n^\varepsilon) \to \bar{p} < \infty$ remains finite in $I(t)$. Then, by (12), we get

$$n^* - n^\varepsilon = O(\varepsilon^{1/\gamma}),$$

and we deduce that

$$\varepsilon n^\varepsilon p'(n^\varepsilon) = O(\varepsilon^{-1/\gamma}) \to \infty.$$

Therefore, in a 'clustering situation' (supposing that the velocity u^ε remains finite as $\varepsilon \to 0$), λ_1^ε tends to $-\infty$. Letting $\lambda_1^\varepsilon \to -\infty$ in the velocity equation

$$\partial_t u^\varepsilon + \lambda_1^\varepsilon \partial_x u^\varepsilon = 0,$$

and supposing that $\partial_t u^\varepsilon$ remains finite implies that the limit velocity u satisfies

$$\partial_x u = 0, \text{ in any interval such that } n = n^*.$$

Therefore, u is uniform (independent of x) in any cluster interval. Of course, the velocity of the cluster may (and does) vary with time. But any change of the velocity in the cluster instantaneously propagates to the entire cluster.

These considerations are rather formal. However, a family of explicit solutions of the RMAR system is well known: those of the Riemann problem, that is the entropic solutions $(n^\varepsilon, u^\varepsilon)$ of (14), (15) with discontinuous initial data

$$(n^\varepsilon, u^\varepsilon)|_{t=0} = \begin{cases} (n_\ell, u_\ell), & \text{for} \quad x < 0 \\ (n_r, u_r), & \text{for} \quad x > 0 \end{cases}. \tag{22}$$

Furthermore, by Godunov's method, we know that any entropy solution of the RMAR system can be obtained from solutions of this kind. Therefore, by looking

at the behavior of such solutions as $\varepsilon \to 0$, we have access to a better knowledge of the CPGD system.

As indicated in the Introduction, this is the goal of Section 6, whose main results are summarized in Section 6.4.1. The reader is advised to skip this Section at the first reading, and to read it later on for checking the details of the most interesting cases (clusters, vacuum etc ...), when reading the sequel of the paper.

4. A rigorous existence result for the CPGD system

The goal of this section is to give a rigorous existence result of weak solutions for the CPGD system. The proof relies on the observation (see [3]) that any smooth function can be approximated, in the distributional sense, by a sequence of characteristic functions. The characteristic function $\mathbf{I}_A$ of a measurable set A takes the value 1 in A and 0 otherwise. In our approach, only measurable sets A consisting of a finite (or at most countable) union of disjoint intervals will be chosen.

Let us consider smooth initial data n^0 and u^0. We can approximate n^0 by n^* times the characteristic function of such a union of intervals. Similarly, n^0u^0 can be approximated using the same union of intervals. Each of these intervals makes an individual cluster which moves freely until it collides with another cluster. In this occurence, the rule which has been outlined in Section 6.4.1 is applied, namely, the fastest cluster which catches up with a slower cluster in front instantaneously takes the velocity of the slowest one. In the present section, we show first that these 'cluster dynamics' realize a weak solution of the CPGD system and second, that such solutions can be used to construct solutions to the CPGD system with arbitrary initial data.

We recall that the CPGD system is given by (18)–(20). We first define the cluster dynamics in Section 4.1 and analyze its properties in Section 4.2. Then, we develop the existence result in Section 4.3.

4.1. Cluster dynamics

Cluster dynamics were first introduced (under the name of 'sticky blocks') in [6] to model the dynamics of gas occlusions in pipes. Sticky blocks have been used to get existence results for various models with constraints in [3, 4]. In this section, we present cluster (or sticky block) dynamics which solve system (18)–(20).

Let us consider a density $n(x,t)$ and a flux $n(x,t)u(x,t)$ given by

$$n(x,t) = \sum_{i=1}^{N} n^* \mathbf{I}_{a_i(t)<x<b_i(t)}, \quad n(x,t)u(x,t) = \sum_{i=1}^{N} n^* u_i(t) \mathbf{I}_{a_i(t)<x<b_i(t)}, \tag{23}$$

with $a_1(t) < b_1(t) < a_2(t) < b_2(t) < \cdots < b_N(t)$. The number of blocks N depends on t, but is piecewise constant. As long as the blocks do not collide, they move at constant velocity $u_i(t)$. When two blocks collide at a time t^*, the density n is given locally by

$$n(x,t) = \begin{cases} n^* \mathbf{I}_{a_l(t)<x<b_l(t)} + n^* \mathbf{I}_{a_r(t)<x<b_r(t)} & \text{if } t < t^*, \\ n^* \mathbf{I}_{a(t)<x<b(t)} & \text{if } t > t^*, \end{cases} \tag{24}$$

and the flux nu by

$$nu(x,t) = \begin{cases} n^* u_l \mathbf{I}_{a_l(t)<x<b_l(t)} + n^* u_r \mathbf{I}_{a_r(t)<x<b_r(t)} & \text{if } t < t^*, \\ n^* u_r \mathbf{I}_{a(t)<x<b(t)} & \text{if } t > t^*, \end{cases} \tag{25}$$

where $a_l(t) = a^* + u_l(t - t^*)$, $b_l(t) = x^* + u_l(t - t^*)$, $a_r(t) = x^* + u_r(t - t^*)$, $b_r(t) = b^* + u_r(t - t^*)$, $a(t) = a^* + u_r(t - t^*)$ and $b(t) = b^* + u_r(t - t^*)$, with $n^* \mathbf{I}_{a^*<x<x^*}$ and $n^* \mathbf{I}_{x^*<x<b^*}$ the two involved blocks at time t^*. The dynamics are exhibited in the following Fig. 1.

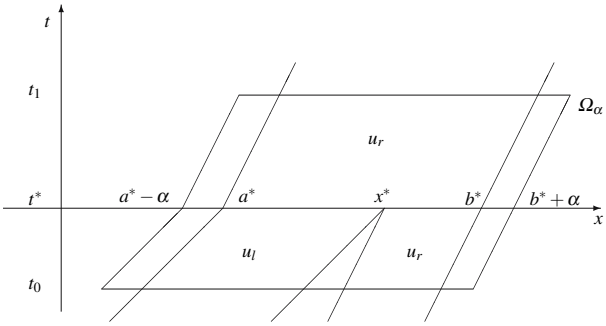

Fig. 1. Sketch of the dynamics when two blocks collide

In a collision, the second block intantaneously takes the velocity of the first one. We extend this when more than two blocks collide at a time t^*, by forming a new block with the velocity of the block on the right of the group.

4.2. Properties of the cluster dynamics

We have the following existence result.

Theorem 1. *There exists a positive function* $\bar{p}(x,t)$ *such that with* $n(x,t)$ *and* $u(x,t)$ *defined by* (23)*, and with the above defined dynamics, we get a solution to* (18)–(20).

Proof. As long as there is no collision, each block moves at a constant velocity u_i, and (n,u) solves the pressureless Euler system. In a neighborhood of the initial data, the proof is given in [3]. We look at the case of a collision of two blocks at a time t^*. The case of simultaneous collisions of blocks can be treated similarly. There exists $\alpha > 0$ such that only the two blocks concerned in the collision are in the set Ω_α defined by

$$\Omega_\alpha = \{(x,t);\quad (t_0 < t \leqq t^* \text{ and } \mathrm{a}^* + \mathrm{u_l}(\mathrm{t} - \mathrm{t}^*) - \alpha < \mathrm{x} < \mathrm{b}^* + \mathrm{u_r}(\mathrm{t} - \mathrm{t}^*) + \alpha) \\ \text{or } (t^* < t < t_1 \text{ and } \mathrm{a}^* + \mathrm{u_r}(\mathrm{t} - \mathrm{t}^*) - \alpha < \mathrm{x} < \mathrm{b}^* + \mathrm{u_r}(\mathrm{t} - \mathrm{t}^*) + \alpha)\},$$

with the notations of the previous section.

Now, define the value of $u(x,t)$ for all x as follows: u is Lipschitz continuous, $u \equiv u_i(t)$ in each block i, u is extended linearly between two successive blocks, and u is constant at $\pm\infty$.

Let $\varphi(x,t)$ be a smooth function with support in Ω_α. Then, for any continuous function S,

$$
\begin{aligned}
&< \partial_t(nS(u)) + \partial_x(nuS(u)), \varphi > \\
&\quad = - < nS(u), \partial_t\varphi > - < nuS(u), \partial_x\varphi > \\
&\quad = -\int_{t_0}^{t^*} \left(\int_{a_l(t)}^{b_l(t)} n^* S(u_l)(\partial_t\varphi + u_l\partial_x\varphi)\,dx + \int_{a_r(t)}^{b_r(t)} n^* S(u_r)(\partial_t\varphi + u_r\partial_x\varphi)\,dx \right) dt \\
&\qquad - \int_{t^*}^{t_1} \int_{a(t)}^{b(t)} n^* S(u_r)(\partial_t\varphi + u_r\partial_x\varphi)\,dx dt. \qquad (26)
\end{aligned}
$$

Now

$$
\frac{d}{dt}\left[\int_{a_l(t)}^{b_l(t)} \varphi(x,t)\,dx \right] = \int_{a_l(t)}^{b_l(t)} \partial_t\varphi(x,t)\,dx + \varphi(b_l(t),t)\,b_l'(t) - \varphi(a_l(t),t)\,a_l'(t),
$$

and $b_l'(t) = a_l'(t) = u_l$, therefore integrating this relation between t_0 and t^*, we obtain

$$
\begin{aligned}
&-\int_{t_0}^{t^*} \left(\int_{a_l(t)}^{b_l(t)} n^* S(u_l)\partial_t\varphi(x,t)\,dx \right) dt \\
&\quad = -\int_{a^*}^{x^*} n^* S(u_l)\varphi(x,t^*)\,dx + \int_{t_0}^{t^*} n^* S(u_l)u_l\,\varphi(b_l(t),t)\,dt \\
&\qquad - \int_{t_0}^{t^*} n^* S(u_l)u_l\,\varphi(a_l(t),t)\,dt,
\end{aligned}
$$

since

$$
\begin{aligned}
\int_{t_0}^{t^*} \frac{d}{dt}\left[\int_{a_l(t)}^{b_l(t)} \varphi(x,t)\,dx \right] dt &= \int_{a_l(t^*)}^{b_l(t^*)} \varphi(x,t^*)\,dx - \int_{a_l(t^0)}^{b_l(t_0)} \varphi(x,t_0)\,dx \\
&= \int_{a^*}^{x^*} \varphi(x,t^*)\,dx.
\end{aligned}
$$

Furthermore, for a term involving $\partial_x \varphi$, we have directly

$$
\begin{aligned}
&-\int_{t_0}^{t^*} \left(\int_{a_l(t)}^{b_l(t)} n^* S(u_l)\, u_l\, \partial_x \varphi(x,t)\, dx \right) dt \\
&= -\int_{t_0}^{t^*} n^* S(u_l) u_l\, \varphi(b_l(t),t)\, dt + \int_{t_0}^{t^*} n^* S(u_l) u_l\, \varphi(a_l(t),t)\, dt.
\end{aligned}
$$

We perform similar computations on the other terms of (26) and we get

$$
< \partial_t (nS(u)) + \partial_x (nuS(u)), \varphi >= \int_{a^*}^{x^*} n^* (S(u_r) - S(u_l)) \varphi(x,t^*)\, dx,
$$

that is

$$
\partial_t (nS(u)) + \partial_x (nuS(u)) = \delta(t-t^*)\, n^*\, (S(u_r) - S(u_l))\, \mathbf{I}_{[a^*,x^*]}(x) \equiv Q^S. \quad (27)
$$

For $S \equiv 1$, we obtain the mass conservation equation and for $S(v) = v$, we get

$$
\partial_t (nu) + \partial_x (nu^2) = \delta(t-t^*)\, n^*\, (u_r - u_l)\, \mathbf{I}_{[a^*,x^*]}(x) \leqq 0,
$$

we recall that here $u_r > u_l$: there is no collision if $u_l \leqq u_r$. Now if we define

$$
\begin{cases} n\bar{p}(x,t) = H(t-t^*)\, n^*\, (u_l - u_r)\, \mathbf{I}_{[a^*,x^*]}\, (x - u_r(t-t^*)), \\ n\bar{p}u(x,t) = u_r\, H(t-t^*)\, n^*\, (u_l - u_r)\, \mathbf{I}_{[a^*,x^*]}\, (x - u_r(t-t^*)), \end{cases} \quad (28)
$$

where H is the Heaviside function, we obtain system (18)–(20). □

Like in the model treated in [6], we have

$$
\frac{u_i(t) - u_{i-1}(t)}{a_i(t) - b_{i-1}(t)} \leqq \frac{1}{t} \text{ for } 2 \leqq i \leqq N. \quad (29)
$$

Indeed, since the blocks $i-1$ and i are disjoint at time t, they have never met before this time. The right boundary of the block $i-1$ is locally given by $b_{i-1}(s) = b_{i-1}(t) + u_{i-1}(t)(s-t)$ and the left boundary of the block i is locally given by $a_i(s) = a_i(t) + u_i(t)(s-t)$. Thus $b_{i-1}(0) < a_i(0)$, even if these blocks come from previous aggregations of blocks. In other words, $b_{i-1}(t) - u_{i-1}(t)t < a_i(t) - u_i(t)t$ which is the announced relation.

Therefore, the above cluster dynamics satisfy the Oleinik condition

$$
\partial_x u(x,t) \leqq \frac{1}{t}, \quad (30)
$$

since $\partial_x u(x,t)$ is exactly given by the left-hand side of (29) between the blocks $i-1$ and i, or 0 on a block and at $\pm\infty$. This condition is important in the pressureless gas dynamics to ensure the uniqueness in the duality sense of [7]. (For the system

of pressureless gas, we also refer to [5, 8, 12, 14]). The Oleinik condition also provides some compactness in x for the velocity u, (see next section.)

Notice that we also have the maximum principle

$$\operatorname*{essinf}_y u^0(y) \leqq u(x,t) \leqq \operatorname*{esssup}_y u^0(y), \tag{31}$$

where essinf and esssup designed the essential inf and the essential sup. We also need to define $\bar{p}$, where $n = 0$. As u, $\bar{p}$, is Lipschitz continuous, $\bar{p} \equiv \frac{n\bar{p}}{n}$ in each block and $\bar{p}$ is extended linearly between two successive blocks, and $\bar{p}$ is constant at $\pm\infty$. If we assume that $u^0 \in BV$, then for any $t \in [\delta, T]$:

$$TV_K(\bar{p}(.,t)) \leqq 2TV_{\tilde{K}}(u^0), \tag{32}$$

for any compact $K = [a,b]$ and with $\tilde{K} = [a - t \operatorname{esssup}|u^0|, b + t \operatorname{esssup}|u^0|]$, where TV_K is the total variation on the set K. We also have the bound

$$0 \leqq \bar{p}(x,t) \leqq \operatorname*{esssup}_y u^0(y). \tag{33}$$

Remark 1. In fact, (30) is valid for any initial data $u^0 \in L^\infty$, which provides a control of $TV(p)$ for any $t \geqq 0$ whenever $\overline{p}(0^+)$ is a BV function. It should be possible - and interesting - to study the case where $\overline{p}(0^+)$ is *not* in BV.

Remark 2. We finally observe that from (27), we have

$$\partial_t(nS(u) + n\bar{p}^S) + \partial_x(nuS(u) + nu\bar{p}^S) = 0, \tag{34}$$

with

$$n\bar{p}^S(x,t) = H(t - t^*)\, n^* \, (S(u_l) - S(u_r))\, \mathbf{I}_{[a^*,x^*]}(x - u_r(t - t^*)),$$

on the set Ω_α. We define $\bar{p}^S(x,t)$ for any x by the same way as $\bar{p}$. We notice that for any compact $K = [a,b]$, we have,

$$TV_K(\bar{p}^S(.,t)) \leqq 2\,\|S'\|_{L^\infty(\tilde{K}_0)} TV_{\tilde{K}}(u^0), \tag{35}$$

with $\tilde{K}_0 = [\operatorname{essinf} u^0, \operatorname{esssup} u^0]$ and $\tilde{K} = [a - t \ \operatorname{esssup}|u^0|, b + t \ \operatorname{esssup}|u^0|]$, for any $S \in C^1(\mathbb{R})$.

4.3. Existence of a solution

We have proved the existence of a solution for particular data. Passing to the limit, we are going to obtain a solution for arbitrary initial data, using the following approximation lemma.

Lemma 1. *Let $n^0 \in L^1(\mathbb{R})$ such that $0 \leqq n^0 \leqq n^*$ and $u^0 \in L^\infty(\mathbb{R})$, then there exists a sequence of block initial data $(n_k^0)_{k\geqq 0}$ and $(n_k^0 u_k^0)_{k\geqq 0}$ such that $\int_{\mathbb{R}} n_k^0(x)\,dx \leqq \int_{\mathbb{R}} n^0(x)\,dx$ and $\operatorname{essinf} u^0 \leqq u_k^0 \leqq \operatorname{esssup} u^0$ for which the convergences $n_k^0 \rightharpoonup n^0$ and $n_k^0 u_k^0 \rightharpoonup n^0 u^0$ hold in the distribution sense.*

This result is proved in [3] and is independent of the chosen dynamics. We shall not reproduce the proof here. Now we need a compactness result for a sequence of solutions with regularity

$$n \in L^\infty_t(0,\infty; L^\infty_x(\mathbb{R}) \cap L^1_x(\mathbb{R})), \tag{36}$$

$$u, \bar{p} \in L^\infty_t(0,\infty; L^\infty_x(\mathbb{R})). \tag{37}$$

Proposition 1. *Let us consider a sequence of solutions* $(n_k, u_k, \bar{p}_k)$ *with regularity* (36)–(37)*, satisfying* (18)–(20)*. The corresponding initial data* $(n^0_k, u^0_k, 0)$ *is supposed to satisfy*

$$0 \leqq n^0_k \leqq n^*, \qquad (n^0_k)_{k\geqq 0} \text{ is bounded in } L^1(\mathbb{R}), \tag{38}$$

$$(u^0_k)_{k\geqq 0} \text{ is bounded in } L^\infty(\mathbb{R}) \cap BV(\mathbb{R}). \tag{39}$$

It is assumed that (30)–(33) *hold.*

Then, up to a subsequence, as $k \to \infty$, $(n_k, u_k, \bar{p}_k) \rightharpoonup (n, u, \bar{p})$ *in the following sense*

$$n_k \rightharpoonup n, \qquad u_k \rightharpoonup u, \qquad \bar{p}_k \rightharpoonup \bar{p} \qquad \text{in } L^\infty_{w*}(]0,\infty[\times\mathbb{R}), \tag{40}$$

where (n, u, p)*, with regularity* (36)–(37)*, is a solution to* (18)–(20) *with initial data* $(n^0, u^0, 0)$ *defined by*

$$n^0_k \rightharpoonup n^0 \text{ in } L^\infty_{w*}(\mathbb{R}), \quad \text{and} \quad n^0_k u^0_k \rightharpoonup n^0 u^0 \text{ in } L^\infty_{w*}(\mathbb{R}). \tag{41}$$

The obtained solution also satisfies (30)*,* (31) *and* (33)*.*

In this result, we denote by $L^\infty_{w^*}(\mathbb{R}\times]0,\infty[)$ the space $L^\infty(\mathbb{R}\times]0,\infty[)$ endowed with the weak * topology.

The key point to the proof of this result is passing to the limit in the products and is treated with the following technical lemma (see [3]).

Lemma 2. *It is assumed that* $(\gamma_k)_{k\in\mathbb{N}}$ *is a bounded sequence in* $L^\infty(\mathbb{R}\times]0,T[)$ *that tends to* γ *in* $L^\infty_{w*}(\mathbb{R}\times]0,\infty[)$*, and satisfies for any* $\Gamma \in C^\infty_c(\mathbb{R})$*,*

$$\int_{\mathbb{R}} (\gamma_k - \gamma)(x,t)\Gamma(x)\,dx \to 0, \quad k \to \infty, \tag{42}$$

either i) a.e. $t \in]0,T[$ *or ii) in* $L^1(]0,T[)$*. It is also assumed that* $(\omega_k)_{k\in\mathbb{N}}$ *is a bounded sequence in* $L^\infty(\mathbb{R}\times]0,T[)$ *that tends to* ω *in* $L^\infty_{w*}(\mathbb{R}\times]0,T[)$ *such that for all compact intervals* $K = [a,b]$*, there exists* $C > 0$ *such that for* $\beta = \omega$ *or* $\beta = \omega_k$*, the total variation (in* x*) of* β *over* K *satisfies*

$$TV_K(\beta(.,t)) \leqq C\left(1 + \frac{1}{t}\right) \text{a.e. t.} \tag{43}$$

Then $\gamma_k\omega_k \rightharpoonup \gamma\omega$ *in* $L^\infty_{w*}(\mathbb{R}\times]0,T[)$*, as* $k \to \infty$*.*

This is a result of compensated compactness, which uses the compactness in x for ω_k given by (43) and the weak compactness in t for γ_k given by (42) to pass to the weak limit in the product $\gamma_k \omega_k$.

Proof (Proposition 1). First we have assumed that the sequence $(u_k)_{k \geqq 0}$ is bounded in $L^\infty(]0, \infty[\times\mathbb{R})$. Then, using the time compactness provided by the system and extracting a subsequence if necessary, we can assume that as $k \to \infty$,

$$n_k \to n \text{ in } C([0,T]; L^\infty_{w*}(\mathbb{R})), \qquad n_k(u_k + \bar{p}_k) \to q \text{ in } C([0,T]; L^\infty_{w*}(\mathbb{R})),$$
$$u_k \rightharpoonup u \text{ in } L^\infty_{w*}(]0,\infty[\times\mathbb{R}), \qquad \bar{p}_k \rightharpoonup \bar{p} \text{ in } L^\infty_{w*}(]0,\infty[\times\mathbb{R}),$$
$$n_k^0 \rightharpoonup n^0 \text{ in } L^\infty_{w*}(\mathbb{R}), \quad \text{and} \quad n_k^0 u_k^0 \rightharpoonup m^0 \equiv n^0 u^0 \text{ in } L^\infty_{w*}(\mathbb{R}).$$

For example, we prove the first convergence the following way: from the mass conservation equation, the sequence (n_k) is bounded in $C_t([0,T]; \mathscr{D}'_x)$ (where $\mathscr{D}'_x$ denotes the space of distributions with respect to x, equipped with the weak topology). Moreover, this sequence is also bounded in L^∞. Thus, at least for a subsequence, we get a convergence in $C_t([0,T]; L^\infty_{w*}(\mathbb{R}))$. In other words,

$$\text{for all } \varphi(x), \; sup| \int (n_k u_k - nu)(x,t)\, \varphi(x) dx| \to 0.$$

Now, from the Oleinik estimate, we have

$$\int_{[a,b]} |\partial_x u_k| \leqq 2\frac{b-a}{t} + 2 \sup_k \|u_k^0\|_\infty,$$

thus Lemma 2 gives

$$n_k u_k \rightharpoonup nu \text{ and } n_k(u_k + \bar{p}_k)u_k \rightharpoonup qu \text{ in } L^\infty_{w*}(]0,\infty[\times\mathbb{R}).$$

Using now (32) and Lemma 2, we obtain

$$n_k \bar{p}_k \rightharpoonup n\bar{p} \;\text{ in }\; L^\infty_{w*}(]0,\infty[\times\mathbb{R}).$$

Therefore, we have $q = n\bar{p} + nu$. Thus, we obtain a solution of (18)–(20). The other convergence results are then easy. □

Theorem 2. *Let $n^0 \in L^1(\mathbb{R})$ such that $0 \leqq n^0 \leqq n^*$ and $u^0 \in L^\infty(\mathbb{R}) \cap BV(\mathbb{R})$. Then there exists $(n, u, \bar{p})$ with regularities* (36)–(37) *satisfying* (18)–(20) *with initial data $(n^0, u^0, 0)$. In addition, the solution satisfies*

$$\partial_x u(x,t) \leqq \frac{1}{t}, \tag{44}$$

$$\operatorname*{essinf}_y u^0(y) \leqq u(x,t) \leqq \operatorname*{esssup}_y u^0(y), \tag{45}$$

$$0 \leqq \bar{p}(x,t) \leqq \operatorname*{esssup}_y u^0(y), \tag{46}$$

$$\partial_t(nS(u) + n\bar{p}^S) + \partial_x(nuS(u) + nu\bar{p}^S) = 0 \text{ in }]0,\infty[\times\mathbb{R}, \tag{47}$$

for every $S \in C^1(\mathbb{R})$, where $\bar{p}^S \in L^\infty([0,\infty[\times\mathbb{R})$ satisfies

$$|\bar{p}^S| \leqq \|S'\|_{L^\infty(\tilde{K})} |\bar{p}|, \tag{48}$$

where $\tilde{K} = [\operatorname{essinf}_y u^0, \operatorname{esssup}_y u^0]$.

Proof. We combine the existence result for sticky blocks, the approximation lemma and the compactness result by the following method. Let n_k^0 and $n_k^0 u_k^0$ be the block initial data of Lemma 1 associated to n^0 and $n^0 u^0$. Using Section 5.2, we get $(n_k, u_k, \bar{p}_k)$ with regularity (36)–(37) satisfying (18)–(20) with initial data n^0, u^0 such that properties (30)–(33) hold. We apply the compactness result: up to a subsequence, as $n \to \infty$, $(n_k, u_k, \bar{p}_k) \rightharpoonup (n, u, \bar{p})$, where (n, u, p), with regularity (36)–(37), is a solution to (18)–(20) with initial data n^0, u^0. The obtained solution also satisfies (44)–(46). All we now have to prove are the entropy equalities (47). The following facts hold true up to the extraction of subsequences. The property (35) allows us to apply the above technical lemma. Now, from (34), we have as $n \to \infty$,

$$n_k \bar{p}_k^S \rightharpoonup n \bar{p}^S \text{ in } L^\infty_{w*}(]0, \infty[\times\mathbb{R}), \qquad n_k(S(u_k) + \bar{p}_k^S) \to q^S \text{ in } C([0, T]; L^\infty_{w*}(\mathbb{R})), \tag{49}$$

for any $S \in C^1(\mathbb{R})$. The second convergence result in (49) and the technical lemma given imply

$$n_k(S(u_k) + \bar{p}_k^S)u_k \rightharpoonup q^S u \text{ in } L^\infty_{w*}(]0, \infty[\times\mathbb{R}).$$

We notice that in (27), Q^S is nonpositive if S is increasing and non-negative if S is nonincreasing. Therefore we can write

$$\partial_t(n_k S(u_k)) + \partial_x(n_k S(u_k)u_k) = Q_k^S,$$

where for example Q_k^S are nonpositive measures for S increasing. As a consequence, the sequence of measures $(Q_k^S)_{k\geq 0}$, which is bounded in the space of distributions, is also bounded in the space of bounded measures for any monotonous S.

Now for $\varphi \in C_c^\infty(\mathbb{R})$,

$$\frac{d}{dt}\int_{\mathbb{R}} n_k S(u_k)\varphi(x)\,dx - \int_{\mathbb{R}} n_k S(u_k)u_k\varphi'(x)\,dx = \int_{\mathbb{R}} Q_k^S\varphi(x)\,dx,$$

thus the sequence

$$\left(\int_{\mathbb{R}} n_k S(u_k)\varphi(x)\,dx\right)_{k\in\mathbb{N}} \text{ is uniformly bounded in } BV_t, \tag{50}$$

for any monotonous function S. But any function $S \in C^1(\mathbb{R})$ is the sum of two monotonous functions. Thus (50) is true for any $S \in C^1(\mathbb{R})$. Now, we want to show that

$$n_k S(u_k) \rightharpoonup nS(u) \text{ in } L^\infty_{w*}(]0, \infty[\times\mathbb{R}), \tag{51}$$

for any continuous function S. By a classical density argument, we only have to prove it for $S(v) = v^\ell$. From (50), we have the same kind of convergence as (42) and thus, applying the technical lemma, we obtain by induction on ℓ

$$n_k u_k^\ell \rightharpoonup nu^\ell, \text{ for any } \ell \in \mathbb{N} \text{ in } L^\infty_{w*}(]0, \infty[\times\mathbb{R}).$$

Therefore, we get (51). Finally, by uniqueness of the limit, we conclude that for any S $q^S = nS(u) + n\bar{p}^S$. □

Remark 3. By the maximum principle, we can easily enforce the (essential) constraint $u \geqq 0$ in the model.

5. Numerical simulations of the CPGD system

In this section, we present some numerical simulations of the CPGD system. As a numerical method, we use a version of the 'follow-the-leader' (FL) model adapted to the CPGD system. In some of these simulations, we refer to Section 6 for a detailed description.

As pointed out in [1], the FL model can be viewed as a spatial discretization of the AR model expressed in Lagrangian coordinates. In Section 2, we have given the expression (13) of a modified FL model (MFL) which corresponds to the spatial discretization of the modified AR model (MAR) with modified pressure (12). The RMAR model (14)–(15) is obtained through a rescaling of the MAR model in which the pressure is multiplied by ε. The corresponding rescaled MFL model (or RMFL) therefore has the expression

$$\dot{x}_i = u_i\,, \quad \dot{u}_i = \frac{\varepsilon}{\gamma}\,\frac{u_{i+1} - u_i}{(x_{i+1} - x_i - d)^{\gamma+1}}\,, \tag{52}$$

where again, $d = 1/n^*$. When $\varepsilon \to 0$, at least formally, the RMAR model converges to the CPGD model (18)–(20). Consequently, letting $\varepsilon \to 0$ in the RMFL model (52) leads to a spatial discretization of the CPGD model in Lagrangian coordinates. This statement is not completely obvious because it involves the commutation of two limits ($\varepsilon \to 0$ and the limit of the spatial discretization to 0). However, we shall take it for granted in the present work.

The formal limit $\varepsilon \to 0$ in (52) leads to the following dynamics

$$\dot{x}_i = u_i\,, \quad \begin{cases} \dot{u}_i = 0\,, & \text{if} \quad x_{i+1} - x_i > d \\ u_i = u_{i+1}\,, & \text{if} \quad x_{i+1} - x_i = d \end{cases}, \tag{53}$$

which will be referred to as the 'constrained follow-the-leader' model (CFTL). This is indeed the model we are going to approximate numerically. In this particle model, vehicles react to the presence of the leading car only when they reach the minimal distance d. They react by instantaneously adjusting their velocity to that of the leading car. When a sequence of vehicles $x_i, x_{i+1}, \ldots, x_{i+p}$ is such that the car seperation is constant equal to d, they form a cluster. The velocity of the cluster is that of the leading car x_{i+p}. Therefore, the CFTL model appears as a very simple and straightforward illustration of CPGD dynamics. We shall use it to produce numerical simulations of CPGD model. Our numerical scheme is based on a simple first order Euler discretization of (53) since we aim at a qualitative understanding of the models rather than at a quantitatively efficient method.

First we report on two simulations related to two different cases of Riemann problems. Then, we consider an example of cluster formation starting from a fairly generic initial situation. The last example refers to the simulation of a bottleneck. The maximal velocity is taken equal to 1 and the maximal density is $n^* = 1$.

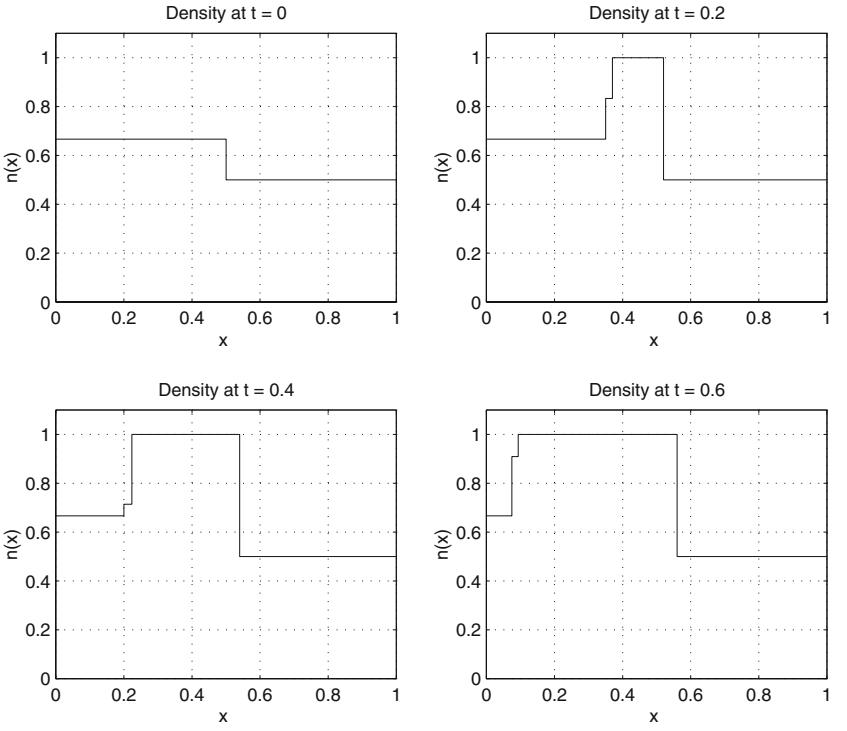

Fig. 2. Riemann problem. Subcase AI.

Riemann problem. We intend to recover some of the results and behaviors described in details in Section 6. Subcases AI and AIII are chosen as references. We consider a portion of road described by the interval $[0, 1]$ and assume that the initial density and velocity are discontinuous at $x = 0.5$ with values of the density to the left and to the right of the discontinuity respectively equal to $n_\ell = 0.7$ and $n_r = 0.5$.

Subcase AI: the initial values of the velocities are $u_\ell = 0.5$ on the left and $u_r = 0.1$ on the right. Fig. 2 shows the density versus space at given (fixed) times. As expected, the left and right states are separated by an expanding cluster. We can check that the right boundary of the cluster moves with velocity u_ℓ while the left boundary moves with the velocity σ given by (64). With the chosen numerical values, $\sigma \sim -0.8$.

Subcase AIII: the initial values of the velocities are $u_\ell = 0.1$ on the left and $u_r = 0.5$ on the right. Fig. 3, showing the density as a function of position at given (fixed) times, confirms that a vacuum appears between the two states. Again, we check that the vacuum region is adjacent on its left and its right to two contact discontinuities moving with speed u_ℓ and u_r respectively. Besides we mention that,

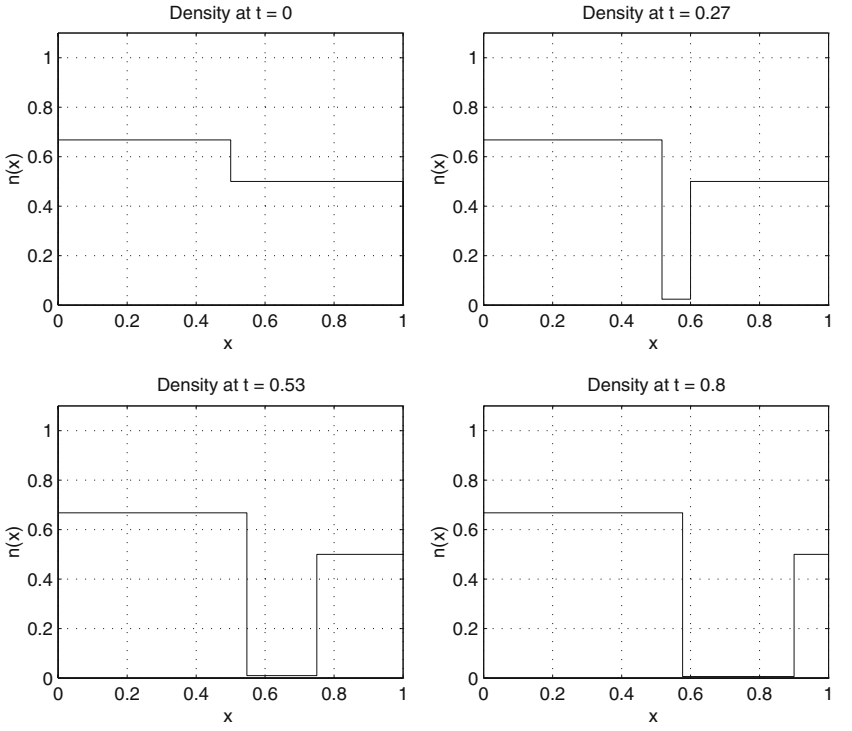

Fig. 3. Riemann problem. Subcase AIII.

as pointed out by DAGANZO in [11], a 'classical' macroscopic model of traffic flow, the Payne–Whitham model [21, 22] would produce negative velocities in this case, while our model does not show this drawback since the velocities do not change during the evolution.

Cluster formation. We consider the evolution of traffic starting from a situation where the vehicles are uniformly distributed along the road with random velocities. The velocity distribution is a normal distribution with average velocity 0.7 and variance 0.2. Vehicles run along a one lane road described by the interval [0, 10]. Periodic boundary conditions are imposed, which amounts to assuming that the road is actually a ring.

Fig. 4 shows the density as a function of position at given (fixed) times. The initially homogeneous situation rapidly leads to the formation of a large number of clusters due to the differences in the vehicle velocities. Then clusters aggregate according to the rules outlined in Section 6. Eventually, a single cluster of vehicles is formed behind the slowest car and moves uniformly.

Fig. 5 gives some information on the statistics of the clusters and its dynamical evolution. The two graphs at the top show the number of clusters divided by the total number N of vehicles versus time (top left figure), and the number of clusters versus time (top right figure). At the beginning there is no cluster in the ring;

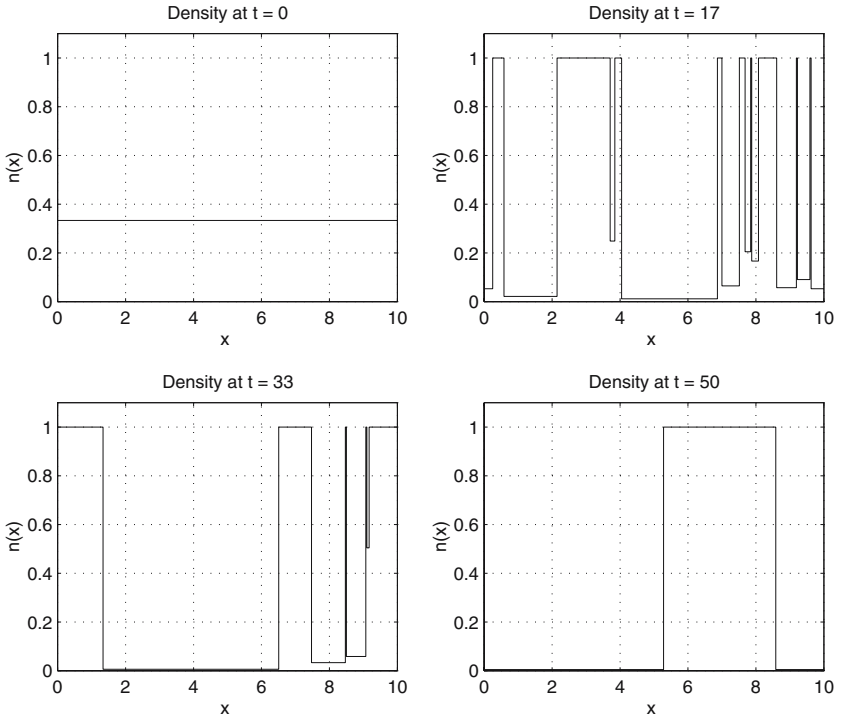

Fig. 4. Cluster formation.

then the number of clusters grows as time goes on and finally decreases, due to aggregation, to the asymptotic value 1. The graphs at the bottom show the average length of the clusters (bottom left figure) and the variance of the cluster length (bottom right figure). The average length of the clusters increases as time goes on and, asymptotically, reaches the value N times the minimal distance between the cars (i.e. N/n^* where n^* is the cluster density), which characterizes the length of the ultimate cluster. The variance of the distribution of cluster lengths goes asymptotically to zero as time goes to infinity.

Fig. 6 shows the velocity distribution of the vehicles. The average velocity (top left figure) decreases with time and the asymptotic value for large times coincides with the velocity of the slowest car. The velocity variance (top right figure) also decays in time and converges to 0 for large times. The bottom figures show the initial and final distribution of velocities (bottom left and bottom right figures respectively). The initial velocity distribution is the prescribed normal distribution, while the final one corresponds to all cars having the same velocity (that of the slowest car).

Bottleneck. We consider traffic on a highway described by the interval [0, 10], with a bottleneck located in [5, 10]. The bottleneck is simulated by reducing the maximal allowed density n^* to half the value allowed on the highway, simulating a reduction from two to one lane. Initially, the vehicles are homogeneously distributed in the

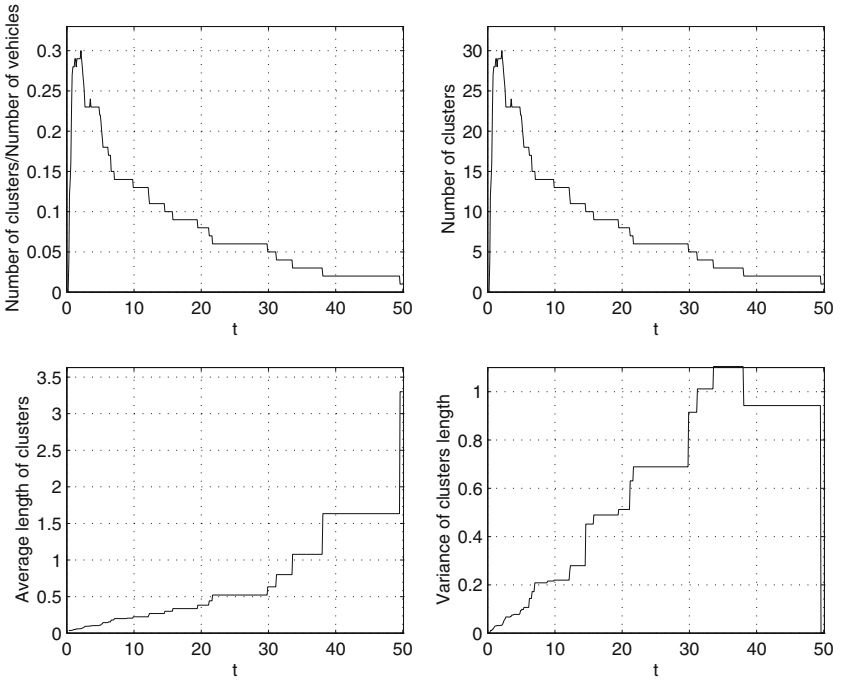

Fig. 5. Clusters statistics.

interval [0, 5] with the same velocity. The initial density is slightly above the maximal allowed density in the bottleneck. When the vehicles reach the bottleneck, only a part of them can get through. Thus the density increases upstream the bottleneck. When the maximal density is reached, the cluster starts to propagate backwards as vehicles pile up. It is separated from the upstream unclustered flow by a cluster terminal shock moving backwards.

Fig. 7 shows various snapshots of the density of vehicles as a function of position. They demonstrate that the simulations reproduce the expected qualitative behavior of the solution fairly well.

6. The Riemann problem for the CPGD system

From the basic theory of nonlinear hyperbolic equations [10, 24, 25], we know that solutions of the Riemann problem consist of simple waves associated with each one of the two characteristic velocities of the system. In this section, we first recall the expressions of the simple waves and of the solutions of the Riemann problem for the RMAR system (14), (15) (Section 6.1). Then, taking the limit $\varepsilon \to 0$, we deduce the expression of the simple waves for the CPGD system (18)–(20) (Section 6.2) and give the solution of the Riemann problem for the CPGD system (Section 6.3). We then develop some consequences of this analysis is Section 6.4.

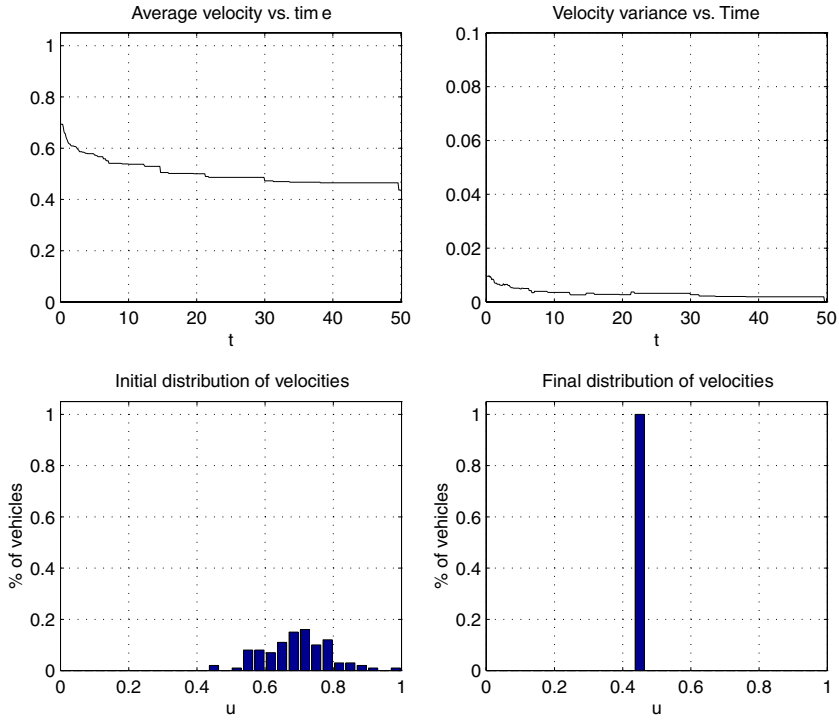

Fig. 6. Velocity distribution.

In the numerous cases of Riemann problems studied below, in order to get a geometric intuition, the reader is advised to draw in each case a picture (in the n, u plane, with a small ε) of the corresponding simple waves of the solution of the RMAR system.

6.1. The Riemann problem for the RMAR system (14), (15)

The characteristic velocities of the RMAR system are given by (21). Since λ_1^ε is genuinely nonlinear, the associated simple waves are either shocks or rarefaction waves. The second eigenvalue λ_2^ε being linearly degenerate, the associated simple waves are contact discontinuities.

6.1.1. Simple waves of the RMAR system. We refer to [2] for the details of the derivation and simply give the results:

($\imath$) First characteristic field: the 1-Shocks or 1-Rarefaction waves are obtained when (n_r, u_r) is connected with (n_ℓ, u_ℓ) through the 1-Wave curve

$$u_r + \varepsilon p(n_r) = u_\ell + \varepsilon p(n_\ell)\,. \tag{54}$$

If $n_r > n_\ell$ (resp. $n_r < n_\ell$), the 1-Wave is a 1-Shock (resp. a 1-Rarefaction wave).

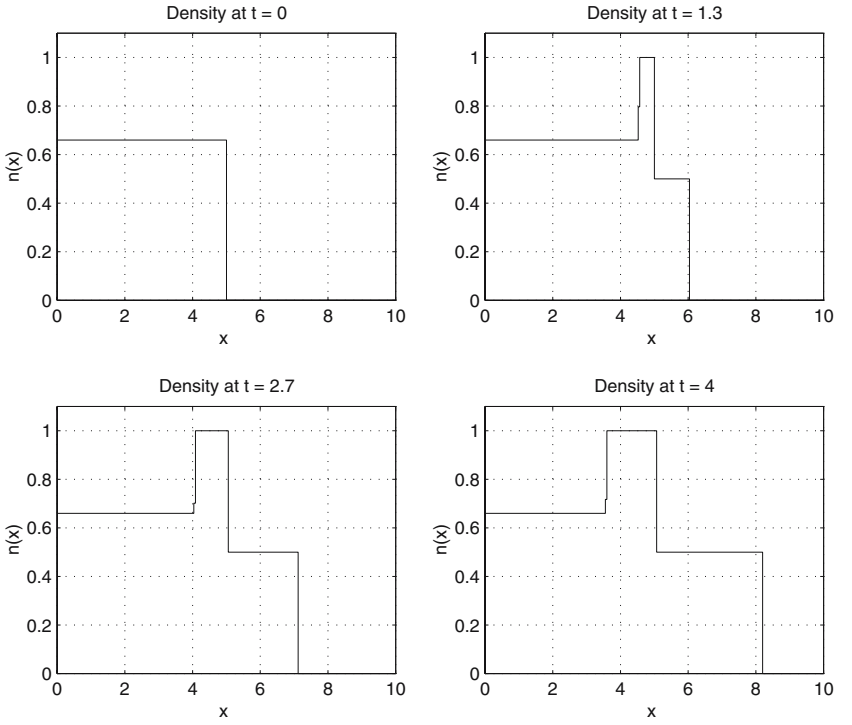

Fig. 7. Bottleneck.

(ι-a) 1-Shocks: they consist of a jump discontinuity between (n_ℓ, u_ℓ) and (n_r, u_r) traveling with a speed σ given by

$$\sigma = \frac{n_r u_r - n_\ell u_\ell}{n_r - n_\ell} \,. \tag{55}$$

(ι-b) 1-Rarefaction waves: they are smooth solutions of the form $(\tilde{n}, \tilde{u})(x/t)$ with $(\tilde{n}, \tilde{u})(\xi)$ given by

$$\tilde{n}(\xi) = (p + np')^{-1} \left(p(n_\ell) + \varepsilon^{-1}(u_\ell - \xi) \right) , \tag{56}$$

$$\tilde{u}(\xi) = \frac{1}{(p + np')(\tilde{n}(\xi))} \left[p(\tilde{n}(\xi))\xi + (np')(\tilde{n}(\xi))(u_\ell + \varepsilon p(n_\ell)) \right] , \tag{57}$$

as long as $\xi \in [\xi_\ell, \xi_r]$ with

$$\xi_{r,\ell} = \lambda_1^\varepsilon(n_{r,\ell}, u_{r,\ell}) = u_{r,\ell} - \varepsilon n_{r,\ell} p'(n_{r,\ell}) \,, \tag{58}$$

and

$$(\tilde{n}, \tilde{u})(\xi) = \begin{cases} (n_\ell, u_\ell) & \text{for} \quad \xi < \xi_\ell \,, \\ (n_r, u_r) & \text{for} \quad \xi > \xi_r \,. \end{cases}$$

(u) Second characteristic field: the 2-contact discontinuities are obtained when $u_\ell = u_r$. They consist of a jump discontinuity between the two constant states (n_ℓ, u) to (n_r, u) (denoting by $u = u_\ell = u_r$) moving with the speed u.

6.1.2. Solution of the Riemann problem for the RMAR system. According to the classical theory [10, 24, 25], the general solution of the Riemann problem for the RMAR system (14), (15) consists of two simple waves seperated by an intermediate state $(\tilde{n}, \tilde{u})$. A 1-wave connects (n_ℓ, u_ℓ) to $(\tilde{n}, \tilde{u})$ and a 2-contact discontinuity connects $(\tilde{n}, \tilde{u})$ to (n_r, u_r). The intermediate state is located at the intersection of the 1-wave curve issued from (n_ℓ, u_ℓ) and of the 2-contact discontinuity curve issued from (n_r, u_r). Therefore, it is given by the two equations $\tilde{u} = u_\ell - \varepsilon(p(\tilde{n}) - p(n_\ell))$, $u_r = \tilde{u}$, or

$$\tilde{n} = p^{-1}(p(n_\ell) - \varepsilon^{-1}(u_r - u_\ell)), \quad \tilde{u} = u_r . \tag{59}$$

We note that in the case $u_r > u_\ell$, the equation for $\tilde{n}$ admits a solution if and only if $p(n_\ell) > \varepsilon^{-1}(u_r - u_\ell)$, that is if $u_r < u_\ell + \varepsilon p(n_\ell)$. In the converse situation, a vacuum appears as shown below. We can therefore distinguish three cases:

Case I: $u_r < u_\ell$. The solution of the Riemann problem consists first of a 1-shock connecting (n_ℓ, u_ℓ) to $(\tilde{n}, u_r)$ and then a 2-contact discontinuity connecting $(\tilde{n}, u_r)$ to (n_r, u_r). We shall write schematically

$$(n_\ell, u_\ell) \quad \overset{1-S}{\longrightarrow} \quad (\tilde{n}, u_r) \quad \overset{2-CD}{\longrightarrow} \quad (n_r, u_r) . \tag{60}$$

Case II: $u_\ell < u_r < u_\ell + \varepsilon p(n_\ell)$. A 1-rarefaction wave connects (n_ℓ, u_ℓ) to $(\tilde{n}, u_r)$ and then a 2-contact discontinuity connects $(\tilde{n}, u_r)$ to (n_r, u_r). We shall write schematically

$$(n_\ell, u_\ell) \quad \overset{1-RW}{\longrightarrow} \quad (\tilde{n}, u_r) \quad \overset{2-CD}{\longrightarrow} \quad (n_r, u_r) . \tag{61}$$

Case III: $u_\ell + \varepsilon p(n_\ell) < u_r$. A 1-rarefaction wave connects (n_ℓ, u_ℓ) to $(0, \tilde{u})$ with

$$\tilde{u} = u_\ell + \varepsilon p(n_\ell) . \tag{62}$$

Then a vacuum appears and finally a 2-contact discontinuity connects the vacuum $(0, u_r)$ to (n_r, u_r). We shall write schematically

$$(n_\ell, u_\ell) \quad \overset{1-RW}{\longrightarrow} \quad (0, \tilde{u}) \quad \overset{Vac}{\longrightarrow} \quad (0, u_r) \quad \overset{2-CD}{\longrightarrow} \quad (n_r, u_r) . \tag{63}$$

In the following sections, we investigate how these simple waves and solutions of the Riemann problem behave in the limit $\varepsilon \to 0$.

6.2. Simple waves of the CPGD system (18)–(20)

In taking the limit when $\varepsilon \to 0$, we must distinguish between several cases according to whether the densities of the initial states (22) (which may depend on ε) tend to the density constraint n^* or not. We suppose that $(n_\ell^\varepsilon, u_\ell^\varepsilon) \to (n_\ell, u_\ell)$ and $(n_r^\varepsilon, u_r^\varepsilon) \to (n_r, u_r)$, where, if $n_{\ell,r} = n^*$, we assume that $\lim \varepsilon p(n_{\ell,r}^\varepsilon) = \bar{p}_{\ell,r}$ with $0 < \bar{p}_{\ell,r} < \infty$. We now successively investigate the two classes of simple waves in all possible cases. Since the value of $\bar{p}$ is important for this discussion,

to each state we shall attach three quantities: the density and velocity as usual, and additionally the value of $\bar{p}$, with the constraint that $\bar{p}(n^* - n) = 0$.

(ι-a) First characteristic field, 1-Shocks: this case only occurs if $n_r \geqq n_\ell$.

Case A: $n_\ell < n^*$, $n_r < n^*$. Then, taking the limit $\varepsilon \to 0$ in (54), we get $u_\ell = u_r$. This is a contact discontinuity of the PGD system.

Case B: $n_\ell = n^*$, $n_r < n^*$. This case does not apply to 1-shocks.

Case C: $n_\ell < n^*$, $n_r = n^*$. Then, taking the limit $\varepsilon \to 0$ in (54), we get $u_\ell = u_r + \bar{p}_r$. This is a 1-shock between $(n_\ell, u_\ell, \bar{p}_\ell = 0)$ and $(n^*, u_r, \bar{p}_r)$ traveling with a speed σ given by

$$\sigma = \frac{n^* u_r - n_\ell u_\ell}{n^* - n_\ell}\,. \tag{64}$$

We can check that $\sigma < u_r < u_\ell$. This situation models the tail of the cluster which propagates upstream: as faster cars enter the cluster, their velocity suddenly decreases, whilst their density increases to the saturation density n^*. The shock moves upstream at a speed determined in a such a way that the in- and outgoing fluxes to the shock are equal. We shall refer to these waves as 'cluster terminal shocks'.

Case D: $n_\ell = n^*$, $n_r = n^*$, with $\bar{p}_r > \bar{p}_\ell$. Then, (54) gives $u_\ell + \bar{p}_\ell = u_r + \bar{p}_r$. Supposing that $u_\ell \neq u_r$ (the equality case being that of a 2-contact discontinuity) and taking the limit $\varepsilon \to 0$ in (55), we obtain that $\sigma = -\infty$. Therefore, as soon as $t > 0$, the solution consists of a constant state $(n^*, u_r, \bar{p}_r)$. This case models the contact of two clusters, the left one being faster than the right one. As soon as contact occurs, the velocity of the left cluster instantaneously adjusts to that of the right one while $\bar{p}$ becomes constant thoughout the union of the two clusters. This type of solution will be referred to as a 'cluster contact'. They will be exploited in the theoretical study below.

(ι-b) First characteristic field, 1-Rarefaction Waves: this case only occurs if $n_r \leqq n_\ell$.

Case A: $n_\ell < n^*$, $n_r < n^*$. Again, taking the limit $\varepsilon \to 0$ in (54), we get $u_\ell = u_r$. We again find a contact discontinuity of the PGD system.

Case B: $n_\ell = n^*$, $n_r < n^*$. Taking the limit $\varepsilon \to 0$ in (54) and (58), we get $u_r = u_\ell + \bar{p}_\ell$ and $\xi_\ell = -\infty$, $\xi_r = u_r$. Taking $\varepsilon \to 0$ in (56), we deduce that $(p+np')(\tilde{n}^\varepsilon(\xi)) \to \infty$ for $\xi \in (-\infty, u_r)$, which implies that $\tilde{n}^\varepsilon(\xi) \to n^*(\xi)$ in the same interval. Using (12), we note that, as $n \to n^*$, $p(n) = O((n^* - n)^{-\gamma})$, while $np' = O((n^* - n)^{-(\gamma+1)})$. Therefore $p \ll np'$ and $p + np' \sim np'$. Hence, taking the limit $\varepsilon \to 0$ in (57), we obtain that $\tilde{u}^\varepsilon(\xi) \to u_\ell + \bar{p}_\ell = u_r$ (which is independent of ξ) for $\xi \in (-\infty, u_r)$ and, using again (56), that $(np')(\tilde{n}^\varepsilon) = O(1/\varepsilon)$. Finally, since

$p(n) = O((np')^{\gamma/(\gamma+1)})$, we have $\tilde{p}^\varepsilon := \varepsilon p(\tilde{n}^\varepsilon) = O(\varepsilon^{1/(\gamma+1)}) \to 0$. Hence, $\tilde{p} = \lim \tilde{p}^\varepsilon = 0$ for $\xi \in (-\infty, u_r)$. For $\xi > u_r$, we have $(\tilde{n}, \tilde{u}, \tilde{p}) = (n_r, u_r, 0)$.

We note that the left state velocity u_ℓ instantaneously changes to u_r as soon as $t > 0$, and that correlatively, $\bar{p}_\ell$ changes to the value 0. In conclusion, the solution of this case consists first of an instantaneous change from the left state $(n^*, u_\ell, \bar{p}_\ell)$ to the intermediate state $(n^*, u_r, 0)$ followed by a contact discontinuity between the intermediate state and the right-state $(n_r, u_r, 0)$, traveling with the velocity u_r. Since the intermediate state corresponds to a value $\bar{p} = 0$, it corresponds to an 'unclustered state' (although $n = n^*$). We call this kind of solution 'instantaneous declustering'.

Case C: $n_\ell < n^*, n_r = n^*$. This case does not apply to 1-rarefaction waves.

Case D: $n_\ell = n^*, n_r = n^*$, with $\bar{p}_r < \bar{p}_\ell$. Taking the limit $\varepsilon \to 0$ in (54) and (58), we get $u_r + \bar{p}_r = u_\ell + \bar{p}_\ell$ and $\xi_\ell = \xi_r = -\infty$. As soon as t is positive, the solution is equal to the constant state $(n_r, u_r, \bar{p}_r)$. This case again describes a 'cluster contact' where the right cluster is now faster than the left one. The left cluster instantaneously accelerates to adjust to the velocity of the right cluster.

(*u*) Second characteristic field, 2-Contact Discontinuities. In this case, we have $u_\ell = u_r := \tilde{u}$. For this case, there is no need to distinguish between the cases A to D. In each case, the solution is a contact discontinuity propagating at velocity $\tilde{u}$ between the states $(n_\ell, \tilde{u}, \bar{p}_\ell)$ and $(n_r, \tilde{u}, \bar{p}_r)$ where n_r and $\bar{p}_r$ may have arbitrary values relative to n_ℓ and $\bar{p}_\ell$.

6.3. Solution of the Riemann problem for the CPGD system (18)–(20)

We are now letting $\varepsilon \to 0$ in the solution of the Riemann problem for the RMAR system (Section 6.1.2). In analyzing this limit, we shall again have to discuss whether n_ℓ and n_r are smaller than n^* or equal to it (cases A to D of Section 6.2). In each of these cases, we will have a second discussion about the relative position of u_ℓ and u_r (cases I to III of Section 6.1.2). This somewhat technical discussion seems unfortunately unavoidable.

Case A: $n_\ell < n^*, n_r < n^*$. In this case, we have $\bar{p}_\ell = \bar{p}_r = 0$.

Subcase AI. $u_r < u_\ell$. The intermediate state $\tilde{n}^\varepsilon$ given by (59) tends to n^* and simultaneously, $\varepsilon p(n^\varepsilon) \to \bar{p} = u_\ell - u_r$. Therefore, a cluster characterized by $(n^*, u_r, \bar{p} = u_\ell - u_r)$ forms as an intermediate state. It is separated by a cluster terminal shock (CTS) to the left state and by a Contact Discontinuity (CD) to the right state. Diagram (60) is then converted into

$$(n_\ell, u_\ell, 0) \quad \overset{CTS}{\longrightarrow} \quad (n^*, u_r, \bar{p} = u_\ell - u_r) \quad \overset{CD}{\longrightarrow} \quad (n_r, u_r, 0) \tag{65}$$

and the solution is depicted in Fig. 8. The formation of a cluster appears as generic.

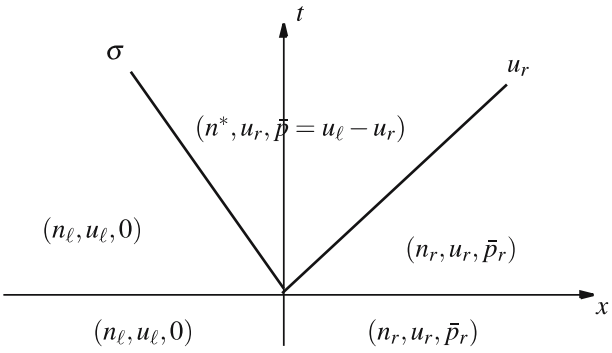

Fig. 8. Cases AI and CI: solution of the Riemann problem in the (x, t)-plane. The intermediate state is a cluster (density n^*) adjacent to a cluster terminal shock of speed σ on the left and a by contact discontinuity of speed u_r on the right. Case AI corresponds to $\bar{p}_r = 0$

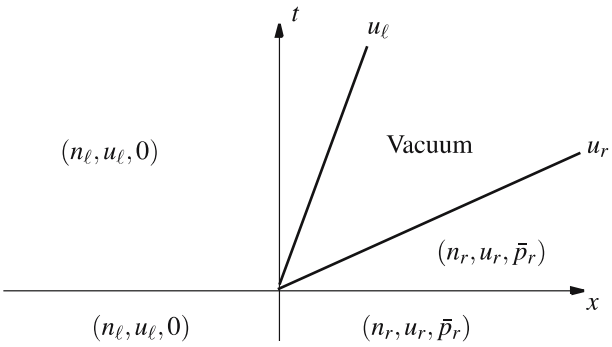

Fig. 9. Cases AIII and CIII: solution of the Riemann problem in the (x, t)-plane. The intermediate state is the vacuum adjacent to two contatct discontinuities of speed u_ℓ on the left and u_r on the right. Case AIII corresponds to $\bar{p}_r = 0$

Subcase AII. This case corresponds to Case II of the discussion of Section 6.1.2. However, since $\bar{p}_\ell = 0$, this case only happens when $u_\ell = u_r$, and is solved by a single contact discontinuity already described in Section 6.2.

Subcase AIII: $u_r > u_\ell$. In this case, a vacuum appears, like in Case III of the RMAR system (see Section 6.1.2). The velocity $\tilde{u}$ which borders the vacuum (62) tends to u_ℓ. Therefore, a contact discontinuity separates the state left state to the vacuum and another contact discontinuity separates the vacuum to the right state. This situation is summarized by the following diagram

$$(n_\ell, u_\ell, 0) \quad \overset{CD}{\longrightarrow} \quad (0, u_\ell, 0) \quad \overset{Vac}{\longrightarrow} \quad (0, u_r, 0) \quad \overset{CD}{\longrightarrow} \quad (n_r, u_r, 0)\,, \qquad (66)$$

and depicted in Fig. 9.

Case B: $n_\ell = n^*$, $n_r < n^*$. In this case, we have $0 < \bar{p}_\ell < \infty$, $\bar{p}_r = 0$.

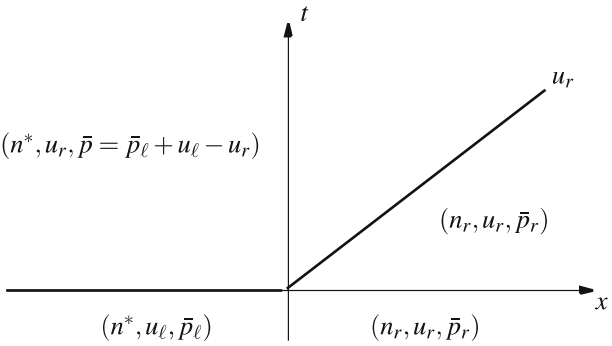

Fig. 10. Cases BI, BII and DI, DII: solution of the Riemann problem in the (x, t)-plane. A transition (cluster contact) immediately takes place between the left state and an intermediate state. The latter is adjacent on its right by a contact discontinuity of speed u_r. Cases BI and BII correspond to $\bar{p}_r = 0$

Subcase BI: $u_r < u_\ell$. Again, the intermediate state $\tilde{n}^\varepsilon$ given by (59) tends to n^* and $\varepsilon p(\tilde{n}^\varepsilon) \to \bar{p} = \bar{p}_\ell + u_\ell - u_r$. Therefore, the first wave is a Cluster Contact (CC) which instantaneously sends the left state $(n^*, u_\ell, \bar{p}_\ell)$ to the intermediate state $(n^*, u_r, \bar{p})$. It is then followed by a contact discontinuity which separates $(n^*, u_r, \bar{p})$ and $(n_r, u_r, 0)$. The diagram is thus

$$(n^*, u_\ell, \bar{p}_\ell) \quad \stackrel{CC}{\Longrightarrow} \quad (n^*, u_r, \bar{p} = \bar{p}_\ell + u_\ell - u_r) \quad \stackrel{CD}{\longrightarrow} \quad (n_r, u_r, 0)\,, \quad (67)$$

where the double arrow indicates that the transition is instantaneous (i.e. the speed of the corresponding wave is $-\infty$). This solution is depicted in Fig. 10.

Subcase BII: $u_\ell < u_r < u_\ell + \bar{p}_\ell$. In this case, the intermediate state $\tilde{n}^\varepsilon$ given by (59) tends to n^* and $\varepsilon p(n^\varepsilon) \to \bar{p} = \bar{p}_\ell + u_\ell - u_r$. Then, the first wave corresponds to a cluster contact (CC) which sends the left state $(n^*, u_\ell, \bar{p}_\ell)$ to the intermediate state $(n^*, u_r, \bar{p})$ followed by a contact discontinuity which relates the intermediate state to the right state $(n_r, u_r, 0)$. The diagram is as follows

$$(n^*, u_\ell, \bar{p}_\ell) \quad \stackrel{CC}{\Longrightarrow} \quad (n^*, u_r, \bar{p} = \bar{p}_\ell + u_\ell - u_r) \quad \stackrel{CD}{\longrightarrow} \quad (n_r, u_r, 0)\,. \quad (68)$$

In this case, the solution is identical with that obtained in the case BI and is again described by Fig. 10.

Subcase BIII: $u_\ell + \bar{p}_\ell < u_r$. There is first an 'Instantaneous Declustering (ID)' wave (see Case B of rarefaction waves in the previous section) which transforms the left state $(n^*, u_\ell, \bar{p}_\ell)$ into an intermediate state $(n^*, u_\ell + \bar{p}_\ell, 0)$. Then a vacuum appears through a contact discontinuity and another contact discontinuity separates the vacuum to the right state $(n_r, u_r, 0)$. The diagram is as follows

$$\begin{aligned}(n^*, u_\ell, \bar{p}_\ell) \quad \stackrel{ID}{\Longrightarrow} \quad (n^*, u_\ell + \bar{p}_\ell, 0) \quad &\stackrel{CD}{\longrightarrow} \quad (0, u_\ell + \bar{p}_\ell, 0) \quad \stackrel{Vac}{\longrightarrow} \quad (0, u_r, 0) \\ &\stackrel{CD}{\longrightarrow} \quad (n_r, u_r, 0)\,, \end{aligned} \quad (69)$$

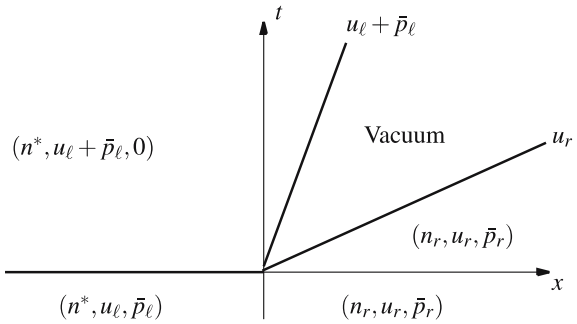

Fig. 11. Cases BIII and DIII: solution of the Riemann problem in the (x, t)-plane. A transition (instantaneous declustering) immediately takes place between the left state and an intermediate state. The latter is adjacent on its right by a vacuum. A contact discontinuity of speed u_r separates the vacuum to the right state. Case BIII correspond to $\bar{p}_r = 0$

and the solution is depicted in Fig. 11.

Case C: $n_\ell < n^*, n_r = n^*$. In this case, we have $0 < \bar{p}_r < \infty$, $\bar{p}_\ell = 0$.

Subcase CI: $u_r < u_\ell$. The intermediate state is $(n^*, u_r, \bar{p} = u_\ell - u_r)$; it is separated from the left state by a cluster terminal shock (CTS) and from the right state by a contact discontinuity. The diagram is the following

$$(n_\ell, u_\ell, 0) \quad \overset{CTS}{\longrightarrow} \quad (n^*, u_r, \bar{p} = u_\ell - u_r) \quad \overset{CD}{\longrightarrow} \quad (n^*, u_r, \bar{p}_r)\,. \tag{70}$$

This situation is analogous to case AI (see Fig. 8).

Subcase CII: In the limit $\varepsilon \to 0$, this case reduces to the case $u_\ell = u_r$ and corresponds to a single contact discontinuity already described in the previous section.

Subcase CIII: $u_\ell > u_r$. Again, a vacuum appears. It is separated from the left state $(n_\ell, u_\ell, 0)$ by a contact discontinuity at velocity u_ℓ and from the right state $(n^*, u_r, \bar{p}_r)$ by another contact discontinuity at velocity u_r. The diagram is as follows

$$(n_\ell, u_\ell, 0) \quad \overset{CD}{\longrightarrow} \quad (0, u_\ell, 0) \quad \overset{Vac}{\longrightarrow} \quad (0, u_r, 0) \quad \overset{CD}{\longrightarrow} \quad (n^*, u_r, \bar{p}_r)\,. \tag{71}$$

This case is analogous to case AIII (see Fig. 9).

Case D: $n_\ell = n^*, n_r = n^*$. In this case, we have $0 < \bar{p}_r < \infty, 0 < \bar{p}_\ell < \infty$.
Subcase DI: $u_r < u_\ell$. The intermediate state is $(n^*, u_r, \bar{p} = \bar{p}_\ell + u_\ell - u_r)$. It is separated from the left state by a cluster contact and from the right state by a contact discontinuity. The diagram is thus

$$(n^*, u_\ell, \bar{p}_\ell) \quad \overset{CC}{\Longrightarrow} \quad (n^*, u_r, \bar{p} = \bar{p}_\ell + u_\ell - u_r) \quad \overset{CD}{\longrightarrow} \quad (n^*, u_r, \bar{p}_r)\,. \tag{72}$$

This case is analogous to case BI (see Fig. 10).

Subcase DII: $u_\ell < u_r < u_\ell + \bar{p}_\ell$. Again, the intermediate state is $(n^*, u_r, \bar{p}_\ell + u_\ell - u_r)$ and is seperated from the left state by a cluster contact and from the right state by a contact discontinuity. The diagram is as follows

$$(n^*, u_\ell, \bar{p}_\ell) \overset{CC}{\Longrightarrow} (n^*, u_r, \bar{p} = \bar{p}_\ell + u_\ell - u_r) \overset{CD}{\longrightarrow} (n^*, u_r, \bar{p}_r)\,. \quad (73)$$

The solution is identical with case DI and analogous with case BII (see Fig. 10).

Subcase DIII: $u_\ell + \bar{p}_\ell < u_r$. Then, like in case BIII, an instantaneous declustering wave appears, followed by a contact discontinuity which connects to a vaccum state. Then, a second contact discontinuity connects the vacuum state to the right state. The diagram is thus

$$(n^*, u_\ell, \bar{p}_\ell) \overset{ID}{\Longrightarrow} (n^*, u_\ell + \bar{p}_\ell, 0) \overset{CD}{\longrightarrow} (0, u_\ell + \bar{p}_\ell, 0) \overset{Vac}{\longrightarrow} (0, u_r, 0) \overset{CD}{\longrightarrow} (n^*, u_r, \bar{p}_r)\,. \quad (74)$$

This case is analogous to case BIII (see Fig. 11).

6.4. Cluster dynamics for the CPGD system

We first synthesize the analysis of the previous section and draw some consequences about the regularity of the solution in the general case (subsection (6.4.1)). We then deduce how $\bar{p}$ can be computed inside the cluster (subsection (6.4.2)). Finally, we investigate how the cluster velocity can be computed (subsection (6.4.3)).

6.4.1. Synthesis of the analysis of the Riemann problem. Certain solutions of the Riemann problem involve an instantaneous transition from the left state to an intermediate state: the corresponding diagrams contain a double arrow, such as (67). These are cases BI, BII, BIII, DI, DII, DIII. We now try to better understand these solutions involving instantaneous transitions.

For this purpose, we group the various cases in two kinds of transitions:

First kind: cases BI and DI. In these cases, a cluster catches up with an unclustered group of vehicles (case BI) or a cluster (case DI) in front, which is **slower**. As the cluster makes contact with this group of vehicles, it instantaneously decelerates and adjusts its velocity to that of the group of vehicles. Simultaneously, the velocity offset $\bar{p}$ in the cluster jumps to a higher value. This kind of jump may happen in this way, not only for solutions of the Riemann problem, but for generic solutions of the CPGD system.

Second kind: cases BII, BIII or DII, DIII. In these cases, a cluster meets an unclustered group of vehicles in front (BII or BIII) or a cluster (DII or DIII), which is **faster**. According to the relative velocity of the two groups of vehicles, either it instantaneously accelerates to the velocity of the vehicles in front, or it accelerates to an intermediate velocity and a vacuum appears between the cluster and the vehicles in front. It can reach the velocity of the vehicles in front only if the velocity offset $\bar{p}$ in the cluster is large enough, so that $\bar{p}$ remains non-negative after the jump.

Otherwise, the intermediate velocity is characterized by the fact that $\bar{p} = 0$ in the cluster after the jump.

In practice, a cluster cannot meet vehicles in front which are faster. So, such solutions of the Riemann problem are 'unphysical' (except maybe at the initial time, but we shall discard it for simplicity). However, a 'smooth' version of these jump dynamics is perfectly physical. Indeed, we can imagine that after each infinitesimal time interval Δt, the cluster velocity makes an infinitesimal jump so as to maintain continuity of the velocity across the right end point of the cluster as long as $\bar{p} \geqq 0$ and otherwise fulfill $\bar{p} = 0$, in which case the cluster is adjacent on its right by a vacuum.

As a consequence of this analysis, we shall assume (in the absence of any rigorous proof of this fact so far) that during smooth phases the cluster always tries to adjust to the maximal velocity allowed by: ($\imath$) the velocity of the cars in front and ($\imath\imath$) the constraint that $\bar{p} \geqq 0$.

To some extent, cases BI and DI of the Riemann problem describe the transition dynamics of the cluster when it catches up with a slower group of vehicles in front. By contrast, cases BII, BIII and DII, DIII are discrete approximations of the dynamics of the cluster when it interacts smoothly with the other vehicles. We now summarize these considerations in the following statement:

Cluster dynamics: we recall that u is independent of x inside a cluster. By contrast, $\bar{p}$ depends on x in general.

($\imath$) **Instantaneous transitions:** they occur when a fast cluster (with velocity u_ℓ) catches up with a slower group of vehicles (with velocity u_r), be it a cluster or an unclustered group of vehicles. At contact, the fast cluster instantaneously adjusts its velocity to the velocity u_r of the slower vehicles in front, while the value of $\bar{p}$ inside the cluster instantaneously jumps to $\bar{p} + u_\ell - u_r$.

(u) **Smooth dynamics:** During smooth phases, one of the two following statements is always true:

(a) $\bar{p} \geqq 0$ inside the cluster and u is continuous across the right end point of the cluster

(b) $\bar{p} = 0$ at the right end point of the cluster and the cluster is adjacent on its right by a vacuum.

The instantaneous transition dynamics of clusters is important. It will allow us to construct sequences of approximate solutions to the CPGD system and to prove the existence of weak solutions of this system in Section 4. We now apply these considerations to compute $\bar{p}$ inside a cluster and the cluster velocity u_c.

6.4.2. Computation of $\bar{p}$ inside a cluster. First, let us define the characteristics $X(t; x, s)$ as the solutions of the ordinary differential equation

$$\frac{dX}{dt}(t) = u(X(t), t), \quad X(s; x, s) = x. \tag{75}$$

$X(t; x, s)$ is nothing but the trajectory of a material particle starting from position x at time s. We consider a cluster occupying the interval $I(t) = [Y_L(t), Y_R(t)]$, i.e. $n = n^*$ in $I(t)$ and $n < n^*$ in a left open neighborhood of $Y_L(t)$ or in a right

open neighborhood of $Y_R(t)$. Denote by $u_c(t)$ the uniform value of $u(x,t)$ in $I(t)$. Equation (19) can be written for $x \in I(t)$:

$$(\partial_t + u\partial_x)\bar{p} + (\partial_t + u\partial_x)u = (\partial_t + u\partial_x)\bar{p} + du_c/dt = 0\,.$$

Since the cluster velocity may have occasional time-jumps, this equation should be understood in the sense of distributions. By integration along the characteristics in the time interval $[t_0, t]$, we get

$$\bar{p}(x,t) + u_c(t) = \bar{p}(x_0,t_0) + u_c(t_0)\,, \tag{76}$$

with $x_0 = X(t_0; x, t)$. Since x belongs to the cluster $I(t)$, we have $\bar{p}(x,t) \geqq 0$. We define $t_0(x)$ as the first time at which the corresponding material particle encounters the cluster. $t_0(x)$ is defined as follows

$$t_0(x) = \min\{\,\tau \ \text{ such that } \ \bar{p}(X(s;x,t),s) > 0\,, \quad \text{a.e. } s \in [\tau, t]\ \}\,.$$

We distinguish between two cases:

Case ($\imath$): $t_0(x) = 0$. Then, initially, $\bar{p}(x_0, 0) \neq 0$. In this case, we get

$$\bar{p}(x,t) = \bar{p}(x_0,0) + u_c(0) - u_c(t), \tag{77}$$

where $\bar{p}(x_0, 0)$ and $u_c(0)$ are given by the initial condition.

Case ($\imath\imath$): $t_0(x) > 0$. The material particle does not belong to a cluster before time t_0 and encounters the cluster at time t_0. For the sake of simplicity, we assume that the cluster velocity u_c does not jump at time t_0. Since $u(X(\cdot; x, t), \cdot)$ and $\bar{p}(X(\cdot; x, t), \cdot)$ may jump at time t_0, (76) must be understood as

$$\bar{p}(x,t) + u_c(t) = \bar{p}(x_0 \pm 0, t_0) + u_c(t_0)\,, \tag{78}$$

where the $+$ sign (resp. $-$ sign) is taken if the particle crosses the left (resp. right) boundary at time t_0. In both cases, the particle velocity $u(X(\cdot; x, t), \cdot)$ may (or may not) have a jump, from its value $u(x_0 \mp 0, t_0)$ before t_0 to the cluster value $u_c(t_0)$. Simultaneously, $\bar{p}(X(\cdot; x, t), \cdot)$ jumps from the value 0 before t_0, to the value $\bar{p}(x_0 \pm 0, t_0)$. According to (19), $(u + \bar{p})(X(\cdot; x, t), \cdot)$ is constant, which implies that

$$u_c(t_0) + \bar{p}(x_0 \pm 0, t_0) = u(x_0 \mp 0, t_0)\,.$$

Inserting this relation into (78), leads to

$$\bar{p}(x,t) = u(x_0 \mp 0, t_0) - u_c(t)\,. \tag{79}$$

It is easy to see that this formula is still valid if u_c has a jump at time t_0.

In (79), $u(x_0 \mp 0, t_0)$ is the velocity of the material particle just before it crosses the boundary of the cluster, i.e., at its preferred velocity. Therefore, the value of $\bar{p}$ inside the cluster is nothing but the velocity offset between the preferred velocity of the corresponding material particle and the actual cluster velocity.

To complete the determination of $\bar{p}$, we need to find the cluster velocity $u_c(t)$. This computation is done in the next section.

6.4.3. Computation of the cluster velocity u_c. From Section (6.4.1) we know how the cluster velocity u_c changes during a catch-up event. We now try to find the law of evolution of u_c during a smooth dynamics phase.

For this purpose, we use the rule that $u(x, t)$ is continuous across the right boundary $Y_R(t)$ of the cluster, except if the latter is adjacent on its right by a vacuum (in which case, $\bar{p}(Y_R(t) - 0, t) = 0$ at the right end point of the cluster). Precisely, we first consider this case, in which (see cases BIII and DIII) there is an instantaneous declustering, followed by a contact discontinuity separating the cluster and the vacuum. Therefore, the interface velocity is equal to the fluid velocity at the interface, that is $dY_R/dt = u(Y_R(t) - 0, t)$, $\bar{p}(Y_R(t) - 0, t) = 0$, and $u + \bar{p}$ is continuous at $x = Y_R(t)$. Differentiating these relations with respect to t and using again (19), we get

$$0 = (\partial_t + u\partial_x)\bar{p}|_{(Y_R(t)-0,t)} = -(\partial_t + u\partial_x)u|_{(Y_R(t)-0,t)} = -du_c/dt$$

(since $\partial_x u = 0$ inside a cluster). Therefore, if a cluster is adjacent on its right by a vacuum, its velocity u_c is constant in time.

We now assume that the cluster is not adjacent to a vacuum, and consequently that $u(x, t)$ is continuous across its right boundary $Y_R(t)$. We now distinguish between two cases according to whether n is continuous or discontinuous across $Y_R(t)$. If n is discontinuous, the discontinuity is a contact discontinuity which propagates at the velocity $dY_R/dt = u(Y_R(t), t)$. Since the points to the right of $Y_R(t)$ do not belong to a cluster, (19) gives

$$0 = (\partial_t + u\partial_x)u|_{(Y_R(t)+0,t)} = (\partial_t + (dY_R/dt)\partial_x)u|_{(Y_R(t)+0,t)} = (d/dt)u(Y_R(t)+0, t).$$

But since $u(x, t)$ is continuous across $Y_R(t)$, we have $u(Y_R(t) + 0, t) = u(Y_R(t) - 0, t) = u_c(t)$ and we deduce that $du_c/dt = 0$. Therefore, if the density is discontinuous at the right end point of the cluster, the cluster velocity is constant.

We now suppose that n is continuous across $Y_R(t)$: $n(Y_R(t) + 0, t) = n^*$ but there is no cluster for $x > Y_R(t)$: in other words, the cluster is "swallowing" the cars ahead, which are just reaching the maximal density. We differentiate this relation with respect to time and get

$$0 = (d/dt)(n(Y_R(t) + 0, t)) = (\partial_t + (dY_R/dt)\partial_x)n|_{(Y_R(t)+0,t)}\,.$$

But, since the points to the right of $Y_R(t)$ do not belong to a cluster, we have

$$((\partial_t + u\partial_x)n + n\partial_x u)|_{(Y_R(t)+0,t)} = 0\,.$$

Taking the difference of these two identities, we obtain

$$((dY_R/dt) - u)\partial_x n|_{(Y_R(t)+0,t)} = (n\partial_x u)|_{(Y_R(t)+0,t)}\,,$$

or

$$\frac{dY_R}{dt} = u(Y_R(t), t) + n^* \frac{(\partial_x u)(Y_R(t) + 0, t)}{(\partial_x n)(Y_R(t) + 0, t)} . \tag{80}$$

We note that $\partial_x u$ and $\partial_x n$ are **not** continuous across $Y_R(t)$ in general and that, in (80), the right limits of these quantities are considered.

Now the cluster velocity is given by $u_c(t) = u(Y_R(t) + 0, t)$, since the velocity is continuous across Y_R. Differentiating this relation with respect to t, we get,

$$du_c/dt = (\partial_t + (dY_R/dt)\partial_x)u|_{(Y_R(t)+0,t)} .$$

But, since the points to the right of Y_R are unclustered, (19) gives

$$(\partial_t + u\partial_x)u|_{(Y_R(t)+0,t)} = 0 .$$

Taking the difference of these two equations, we get, using (80)

$$du_c/dt = ((dY_R/dt - u)\partial_x u)|_{(Y_R(t)+0,t)} = n^* \frac{((\partial_x u)(Y_R(t) + 0, t))^2}{(\partial_x n)(Y_R(t) + 0, t)} . \tag{81}$$

Because n is continuous at $Y_R(t)$ and equal to its maximal value n^* on the left of $Y_R(t)$, we necessarily have $(\partial_x n)(Y_R(t) + 0, t) \leqq 0$. We deduce that $du_c/dt \leqq 0$. Therefore, a cluster can only decelerate and, by (79), $\bar{p}$ can only increase along particle trajectories. Consequently, particles belonging to a cluster can never leave the cluster.

We also have $(\partial_x u)(Y_R(t) + 0, t) \leqq 0$. Indeed, if $(\partial_x u)(Y_R(t_0) + 0, t_0) > 0$ at an instant t_0, by (80) we get $(dY_R/dt)(t_0) < u(Y_R(t_0), t_0) = u_c(t_0)$. But, according to the previous remark, the material particle $X(t; Y_R(t_0), t_0)$ belongs to the cluster at any time $t > t_0$. Therefore, $(dY_R/dt)(t_0) \geqq u(Y_R(t_0), t_0)$, which contradicts the previous inequality.

Consequently, in this situation, the cluster is adjacent on its right to a non zero density and both the velocity and the density are continuous across its right boundary. This case can only occur if $(\partial_x u)(Y_R(t)+0, t) \leqq 0$. In this case, we have $(dY_R/dt)(t_0) \geqq u(Y_R(t_0), t_0) = u_c(t_0)$ which means that the 'head' of the cluster moves faster than the cluster itself. This is easily understood: because cars in front of the cluster are obliged to decelerate, their density increases and eventually they reach the maximal density n^*. At this point, they enter the cluster. Simultaneously, the cluster is forced to decelerate in order to adjust to the velocity of these vehicles in front. This deceleration is measured by (81), and this concludes the section.

7. Conclusion

In this paper, we have presented a traffic flow model which describes the formation and evolution of traffic jams. It consists of a constrained pressureless gas dynamics system deduced from the Aw–Rascle model through a singular limit. Traffic jams or clusters appear as regions where the density constraint is attained and their dynamics are derived through the analysis of the Riemann problem for

the Aw–Rascle model. An existence result of weak solutions for this model is proved by using the cluster dynamics to construct a sequence of approximations. A numerical method based on an appropriate follow-the-leader model is designed and numerical results are shown.

Of course, this model is rather primitive for several reasons: it is a single lane model and therefore does not allow for the possibility that cars could take over the traffic jams. The density constraint is independent of the velocity, whilst a more realistic model should include such a dependence. Finally, the specific events occuring at road junctions would require a specific analysis. Also, numerical strategies based on the direct discretization of the model (rather than passing through a follow-the-leader model) should be designed.

However, it is our belief that the model possesses some basic features which make it interesting for traffic flow modeling. It does not depend on too many phenomenological data and it seems to describe the basic features of cluster dynamics in a correct way. We think that it can serve as the basis for future developments of simple as well as accurate traffic flow models.

Acknowledgements The support of the European network HYKE, funded by the EC as contract HPRN-CT-2002-00282, is acknowledged.

References

1. Aw, A., Klar, A., Materne, A., Rascle, M.: Derivation of continuum traffic flow models from microscopic follow-the-leader models. *SIAM J. Appl. Math.* **63**, 259–278 (2002)
2. Aw, A., Rascle, M.: Resurrection of second order models of traffic flow. *SIAM J. Appl. Math.* **60**, 916–938 (2000)
3. Berthelin, F.: Existence and weak stability for a two-phase model with unilateral constraint. *Math. Models Methods Appl. Sci.* **12**, 249–272 (2002)
4. Berthelin, F., Bouchut, F.: Weak solutions for a hyperbolic systems with unilateral constraint and mass loss. *Ann. Inst. H. Poincare Anal. Non Linéaire* **20**, 975–997 (2003)
5. Bouchut, F.: On zero pressure gas dynamics. In: (Ed. Perthame, B.), *Advances in kinetic theory and computing,* World Scientific (1994)
6. Bouchut, F., Brenier, Y., Cortes, J., Ripoll, J.F.: A hierachy of models for two-phase flows. *J. Nonlinear Sci.* **10**, 639–660 (2000)
7. Bouchut, F., James, F.: Duality solutions for pressureless gases, monotone scalar conservation laws, and uniqueness. *Comm. Partial Differential Equations* **24**, 2173–2189 (1999)
8. Brenier, Y., Grenier, E.: Sticky particles and scalar conservation laws. *SIAM J. Numer. Anal.* **35**, 2317–2328 (1998)
9. Colombo, R.M.: A 2×2 hyperbolic traffic flow model Traffic Hav modelling and simulation. *Math. Comp. Modelling* **35**, 683–688 (2002)
10. Dafermos, C.: *Hyperbolic conservation laws in continuum physics*. Springer-Verlag, 1999
11. Daganzo, C.: Requiem for second order fluid approximations of traffic flow. *Transp. Res. B* **29B**, 277–286 (1995)
12. E, W., Rykov, Y.G., Sinai, Y.G.: Generalized variational principles, global weak solutions and behavior with random initial data for systems of conservation laws arising in adhesion particle dynamics. *Comm. Math. Phys.* **177**, 349–380 (1996)
13. Gazis, D.C., Herman, R., Rothery, R.: Nonlinear follow-the-leader models of traffic flow. *Oper. Res.* **9**, 545–567 (1961)

14. Grenier, E.: Existence globale pour le système des gaz sans pression. *C. R. Math. Acad. Sci. Paris* **321**, 171–174 (1995)
15. Klar, A., Wegener, R.: Traffic flow: models and numerics. In: *Modeling and Computational Methods for Kinetic Equations*, Birkhäuser, Boston, 219–259 (2004)
16. Klar, A., Wegener, R.: Enskog-like kinetic models for vehicular traffic. *J. Stat. Phys.*, **87**, 91–114 (1997)
17. Lighthill, M.J., Whitham, J.B.: On kinematic waves. I: flow movement in long rivers. II: A theory of traffic flow on long crowded roads. *Proc. R. Soc. Lond. Sec A* **229**, Math. Phys. Eng. Sci. 281–345 (1955)
18. Nagel, K., Schreckenberg, M.: A cellular automaton model for freeway traffic. *J. Physique* **2**, 2221–2229 (1992)
19. Nelson, P.: A kinetic model of vehicular traffic and its associated bimodal equilibrium solutions. *Transport. Theory Statist. Phys.* **24**, 383–409 (1995)
20. Paveri-Fontana, S.L.: On Boltzmann-like treatments for traffic flow. *Transportation Res.* **9**, 225–235 (1975)
21. Payne, H.J.: Models of Freeway Traffic and Control. In: *Mathematical Models of Public Systems*, Simulation Council Proc. **1**, (1971)
22. Payne, H.J.: FREFLO: A macroscopic simulation model of freeway traffic. *Transportation Research Record* **722**, 68–75 (1979)
23. Prigogine, I., Herman, R.: *Kinetic theory of vehicular traffic*. American Elsevier Publishing Co, New-York, 1971
24. Serre, D.: *Systems of conservation laws 1 & 2*. Cambridge University Press, 1999 and 2000
25. Smoller, J.: *Shock waves and reaction-diffusion equations*. Springer-Verlag, 1983
26. Temple, B.: Systems of conservation laws with coinciding shock and rarefaction curves. *Contemp. Math.* **17**, 143–151 (1983)
27. Zhang, M.: A non-equilibrium traffic model devoid of gas-like behavior. *Transportation Res. B* **36**, 275–290 (2002)

Laboratoire J. A. Dieudonné,
Université de Nice,
Nice, France.
e-mail: Florent.Berthelin@unice.fr

and

MIP UMR 5640,
Université Paul Sabatier,
Toulouse, France.
e-mail: degond@mip.ups-tlse.fr

and

Department of Mathematics,
Politecnico di Torino,
Torino, Italy.
e-mail: marcello.delitala@polito.it

and

Laboratoire J. A. Dieudonné,
Université de Nice,
Nice, France.
e-mail: rascle@math.unice.fr

(*Received December 31, 2004 / Accepted October 13, 2006*)
Published online November 17, 2007 –